CR 73358

AVAILABLE TO THE PUBLIC

N69-34308

NASA CR-73358

DEVELOPMENT OF A CO_2-H_2O SOLID OXIDE ELECTROLYTE ELECTROLYSIS SYSTEM

by

J. Weissbart and W. H. Smart

S. H. Inami

C. M. McCullough

S. A. Ring

CASE FILE COPY

FIRST ANNUAL REPORT

May 1969

NATIONAL AERONAUTICS AND SPACE ADMINISTRATION

AMES RESEARCH CENTER

Moffett Field, California 94035

Prepared Under Contract No. NAS2-4843

APPLIED ELECTROCHEMISTRY INC.

2425 Leghorn Street

Mountain View, California 94040

DEVELOPMENT OF A CO_2-H_2O SOLID OXIDE ELECTROLYTE ELECTROLYSIS SYSTEM

by
J. Weissbart and W. H. Smart
S. H. Inami
C. M. McCullough
S. A. Ring

FIRST ANNUAL REPORT
May 1969

NATIONAL AERONAUTICS AND SPACE ADMINISTRATION
AMES RESEARCH CENTER
Moffett Field, California 94035

Prepared Under Contract No. NAS2-4843

APPLIED ELECTROCHEMISTRY INC.
2425 Leghorn Street
Mountain View, California 94040

FOREWORD

The research and development work reported here was performed at Applied Electrochemistry Incorporated, Mountain View, California, from March 29, 1968 to May 29, 1969, under Contract NAS2-4843. The work was done by Dr. J. Weissbart, Dr. W. H. Smart, who were the principal investigators, Mr. S. H. Inami, Mr. C. M. McCullough and Mr. S. A. Ring. The project was under the overall direction of Dr. Weissbart. The technical monitor was Dr. T. Wydeven, Environmental Control Research Branch, NASA Ames Research Center, Moffett Field, California.

Distribution of this report is provided in the interest of information exchange. Responsibility for the contents resides in the authors and organization that prepared it.

ABSTRACT

A twelve-ampere multi-cell CO_2-H_2O electrolyzer employing stabilized zirconia electrolyte disks was designed, fabricated, tested and operated to produce O_2 and carbon from CO_2 in conjunction with a catalytic CO disproportionator. Design principles applicable to solid oxide electrolyte devices of this type are presented. These principles include ceramic electrolyte in the form of plates, series electrical connection of cells, parallel gas flows, and gas-tight high-temperature seals. The twelve-ampere prototype used hot-pressed zirconia disks 6.35 cm in diameter and .109 cm thick, platinum electrodes, zirconia cell bodies and gas manifolds, and precious metal brazed seals. The size of each cell, 20 cm^2 of active area, is believed adequate for incorporation into a 127-ampere unit sufficient to supply O_2 for one man (two pounds per day). These cells electrolyzed CO_2 at 825°C without significant electrode polarization in both single cell tests and connected together in the multi-cell unit. Application of data resulting from the fabrication and testing phases of this program to the development of larger units for O_2 recovery from CO_2 for use in aerospace life-support systems is discussed.

CONTENTS

Section		Page
	FOREWORD	ii
	ABSTRACT	iii
	ILLUSTRATIONS	vi
	TABLES	viii
1	INTRODUCTION	1
2	ELECTROLYZER DESIGN	3
	2.1 Design Principles	3
	2.2 Twelve-Ampere Prototype	10
3	FABRICATION OF THE TWELVE-AMPERE ELECTROLYZER	14
	3.1 Electrolyte Disks	14
	3.2 Cell Bodies	24
	3.3 Sealing	31
	3.3.1 Individual Cells	31
	3.3.2 Multi-Cell Units	36
4	CATALYTIC REACTOR	40
5	TESTING	43
	5.1 Single Cells	43
	5.2 Twelve-Ampere Electrolyzer	46
	5.2.1 Experimental Details	46
	5.2.2 Results and Discussion	52

Section		Page
6	DISCUSSION	59
	6.1 Summary of the Development Program	59
	6.2 Present State of This Technology	60
	6.3 Future Development	63
7	REFERENCES	64

ILLUSTRATIONS

Figure		Page
2-1	Solid Oxide Electrolyte Unit Using Ceramic Cell Bodies	5
2-2	Electrolyzer with Metal Structural Parts	6
2-3	Components of the Electrolyzer	8
2-4	Electrolyzer Design with Uniform, Thin Ceramic Walls	9
2-5	Cutaway View of the 12-A Unit	11
2-6	Perspective View of the 12-A Unit	12
2-7	Components of an Individual Cell	13
3-1	Schematic View of the Hot Press and Muffle Tube Assembly (Scale: 2 Inches = 1 Foot)	15
3-2	Blackening of the Outer Rim of a Disk Due to Reduction in the Hot Press	23
3-3	Electrolyte Disk Showing Electrodes and Sealing Rim	25
3-4	Ceramic Cell Body	27
3-5	Top View of a Zirconia Cell	34
3-6	Bottom View of a Zirconia Cell	35
3-7	Twelve-Ampere Electrolyzer	38
3-8	Close-Up of Twelve-Ampere Electrolyzer	39
4-1	Efficiency of the Steel Reactor as a Function of Exposure Time	42
5-1	Single Cell Electrical Testing Arrangement	44
5-2	Comparison of Conductivity of Bulk Hot-Pressed, Cold-Pressed and Sintered, and Thin Film Zirconia-Scandia Electrolytes	45

Figure		Page
5-3	Twelve-Ampere Electrolysis Unit Undergoing Testing	48
5-4	Schematic Diagram of Electrolyzer and Reactor	49
5-5	Schematic Wiring Diagram of 12-A Electrolysis Unit	50
5-6	Schematic for Electrical Measurements	51
5-7	Current-Voltage Curves for Electrolyzer	53
5-8	Current-Voltage Curves for Single Cells in Electrolyzer	55

TABLES

Table		Page
3-1	Hot Pressings - ZrO_2-CaO Powder	17
3-2	Hot Pressings - ZrO_2-Y_2O_3 Powder	18
3-3	Hot Pressings - ZrO_2-Sc_2O_3 Powder	19
3-4	Hot Pressings - MgO Powder	29
3-5	Hot Pressings - Magnesium Silicates	30
3-6	Coefficients of Thermal Expansion (10^7cm/cm-^oC)	36
5-1	Current-Voltage for Oxygen Transfer at 820^oC	54
5-2	Approximate Values of Lead Resistance Losses	54
6-1	Weights of 12-A Unit Components	62

Section 1

INTRODUCTION

A critical problem to be solved for space missions beyond three months is the regeneration of oxygen from the exhaled carbon dioxide in the atmosphere of the space cabin. Feasibility studies and laboratory development work of several chemical processes based on the Sabatier and Bosch reactions for CO_2 conversion and oxygen recovery have been extensively supported for this purpose. Much less work in this area has been done with high temperature solid oxide cells. A qualitative comparison of various systems for the regeneration of O_2 from CO_2 based on the available experimental data and an appraisal of their relative complexity, engineering and system integration difficulties and eventual reliability appropriate for space missions rates the solid oxide electrolyte system very highly. This appraisal has been confirmed by the results achieved on the previously supported NASA/Ames program under contract NAS2-2810, entitled "Study of Electrolytic Dissociation of CO_2-H_2O Using A Solid Oxide Electrolyte" (Refs. 1 and 2). The present program under contract NAS2-4843 has as its primary goal, based on the previously obtained results, the extension of this work to the design, contruction and operation of a multi-cell 12-A electrolysis and catalytic reactor system. The 12-A unit should be able to serve as a sub-system or unit building block for a one-man electrolysis unit.

The magnitude of the scale-up required to achieve the goals of the present NAS2-4843 program is illustrated by a comparison of the 12-A unit with the previously constructed 1-A "lollipop" unit. The requirement under the NAS2-2810 program was the design, construction and operation of a 1-A two-cell laboratory model electrolysis unit operating near 800°C continuously for 1,000 hours at a current density of 100 mA/cm^2 with a CO_2-H_2O mixture. The 1-A unit consisted of two stabilized zirconia electrolyte disks of 4.45 cm diameter and 5 cm^2 active electrode-electrolyte area per disk for a total active area of 10 cm^2. That unit contained one anode and one cathode chamber. The present program required at least three electrolyte disks of 6.35 cm diameter and 20 cm^2 active electrode-electrolyte area per disk for a total active area of 60 cm^2, and a total of four anode and cathode gas

chambers with cell electrical connections in series and cell feed gas connections in parallel. To the electrolyzer must be connected a CO-disproportionation reactor.

To accomplish this task a large-scale expansion in ceramic electrolyte and cell body fabrication cabability from previous NAS2-2810 program levels was undertaken during the year covered by this progress report. Expansion took place in the areas of powder preparation, powder compaction, ceramic machining, drilling and polishing, as well as sealing and electrode preparation with the concomitant requirement of construction, installation and testing of large firing ovens and furnaces, hot-pressing equipment and ceramic machining equipment. Research in support of the development program was also performed.

Three 12-A electrolyzers were built and preliminary tests were made on them. One of these units was operated on CO_2 saturated with H_2O at room temperature in conjunction with a catalytic reactor to deposit carbon from disproportionation of CO from the electrolyzer. In the course of this development program, sufficient knowledge and experience was gained in the areas of zirconia electrolyte fabrication, large high temperature seals, battery construction and manifolding to allow work to proceed to the next step--the construction of a one-man scale (127-A) electrolyzer.

Section 2

ELECTROLYZER DESIGN

2.1 DESIGN PRINCIPLES

A consideration of the goals to be attained by multi-cell solid oxide CO_2 electrolyzers for NASA life-support end use has led to our adoption of a set of guiding principles for their design and construction. Successful designs should permit the evolution of electrolyzers capable of reliable long-term operation under zero-gravity conditions. In addition, these designs must be sufficiently compatible with fabrication technology to permit units to be built and tested on a laboratory scale, to be scaled up later to practical capacities, and to operate at practical current densities, gas flow rates, and thermal parameters without adverse effects on either internal components or on sub-systems to which the electrolyzer is connected.

Design principles formulated in the belief that these goals can be met, and based on extensive background in solid oxide electrochemistry and ceramic technology, can be summarized as follows:

(1) The ceramic electrolyte is in the form of a disk or plate for ease of fabrication and electrode processing.

(2) The electrolyte is a separate component from the cell body segment and does not provide structural support other than for electrodes.

(3) There is accessibility and interchangeability of anode and cathode surfaces for the fabrication of flat, porous electrodes.

(4) The seals are gas-tight, noble metal ceramic-to-ceramic or metal-to-ceramic.

(5) The cells are connected in series electrically obviating high-current conductors and minimizing heat losses due to conduction.

(6) The gas flow to the cells is in parallel to maintain uniform gas composition in each cell preventing preferential chemical reduction and electronic conduction paths in the electrolyte.

(7) Cell segments or bodies have compositions which are essentially unrelated to the composition of the electrolyte disks.

(8) Individual cells can be tested before final assembly.

(9) The number of cells can be increased without major design changes.

(10) The size of cells can be increased without major design changes.

(11) External area to volume ratio is controlled to reduce heat losses via radiation.

(12) Electrolyte disks can be modified by composition, thickness or be replaced by thin supported films without requiring major design modifications.

These design concepts can be adhered to in units with stabilized zirconia electrolyte disks sealed to either ceramic or metal cell segments. An example of a unit using ceramic cell segments is shown in Fig. 2-1 whereas Fig. 2-2 illustrates the use of metal segments. The composition of cell segments need not be related to the composition of the electrolyte. Potential materials include stabilized zirconia, magnesium and aluminum silicates (Lava, Forsterite, Steatite), magnesium oxide, high temperature metals and alloys (Hastelloy, Inconel, Kanthal).

In the design employing ceramic structural parts (Fig. 2-1), the flat ceramic electrolyte disks holding the electrodes are supported by ceramic spacers containing the gas manifolds, gas entry and exit holes, and electrical lead-throughs. One end of the stack is closed with a blank ceramic plate whereas the other end plate contains gas inlet and outlet tubes. Each electrolyte disk with its two sealed-on porous electrodes constitutes one cell. The cells are electrically connected in series by short wires sealed through the ceramic

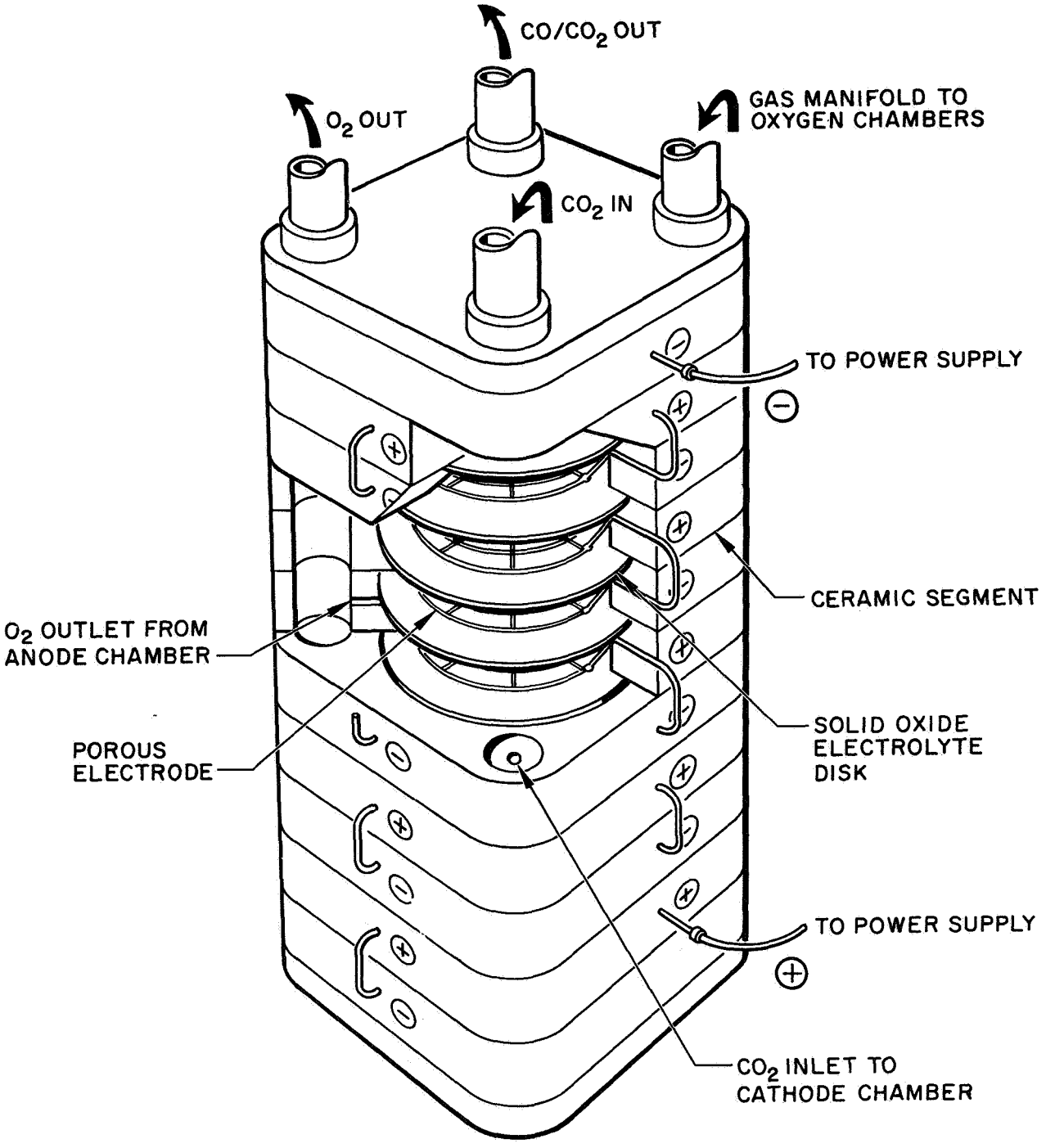

Fig. 2-1 Solid Oxide Electrolyte Unit Using Ceramic Cell Bodies

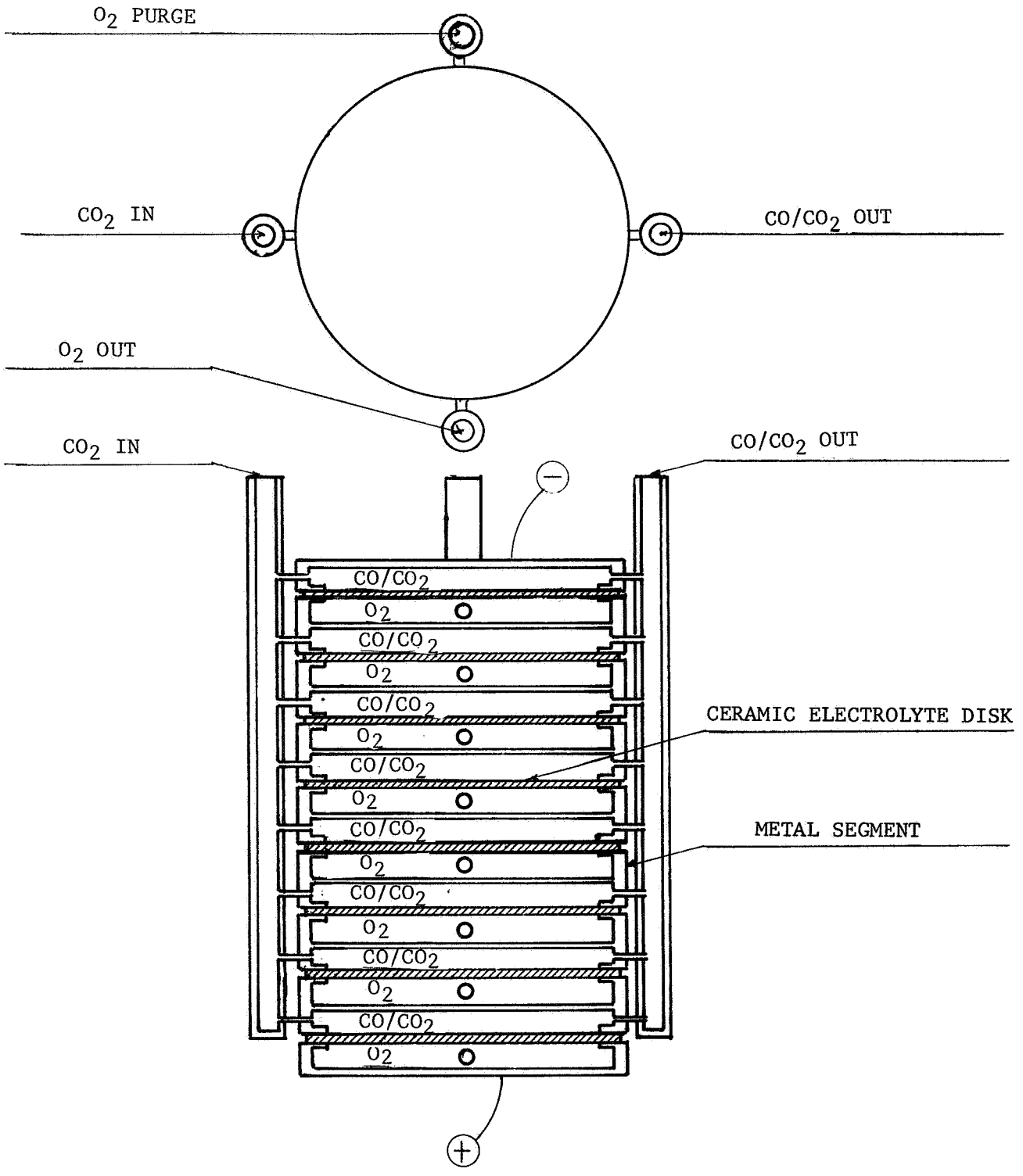

Fig. 2-2 Electrolyzer with Metal Structural Parts

segments. The entire unit contains only four kinds of ceramic components, viz., electrolyte disks with electrodes, spacers, a blank end piece, and an end piece with gas tubes (see Fig. 2-3).

This version of a 12-A unit using ceramic cell bodies is an approach to the design shown in Fig. 2-4 which has uniform, thin ceramic walls. Another variation of this basic design, intermediate between those of Fig. 2-3 and Fig. 2-4 was shown in Fig. 4-1 of Ref. 1. Many other modifications are possible; the choice must depend upon practical ceramic fabrication and sealing technology as well as on desiderata of heat transfer, stress-strain relationships and weight per unit of oxygen output.

In the design shown in Fig. 2-2 the disks are sealed to metal segments containing a septum that divides the space between disks into two gas chambers. The electrodes are in electrical contact with the metal segments which serve to connect the disks in series electrically. This design has the advantage that electrical leads need be brought out only from the end cells, but it suffers the disadvantage of requiring a metal that can be used at high temperature in both oxidizing and reducing atmospheres which is thermally compatible with the ceramic electrolyte. In addition, provision would have to be made to prevent the gas manifolds from short-circuiting the cells, either by using non-conducting manifold materials or by appropriate electrical insulation.

In either modification of the basic design (i.e., structural components of ceramic or of metal) the cells would be electrically connected in series to prevent breakdown that could occur with disks connected in parallel caused by the following sequence of events: a slight imbalance in the current heating one disk causes its resistance to fall because of the negative temperature coefficient of resistance of the electrolyte; this allows more current to flow through that disk until a runaway condition develops in which most of the current in one disk could result in failure of the unit by local overheating and cracking of the electrolyte. With series connection and control of the current, breakdown of this type could not occur.

Although series electrical connection would be mandatory, series flow of gases through the cells would have the disadvantage that the cells would operate under widely differ-

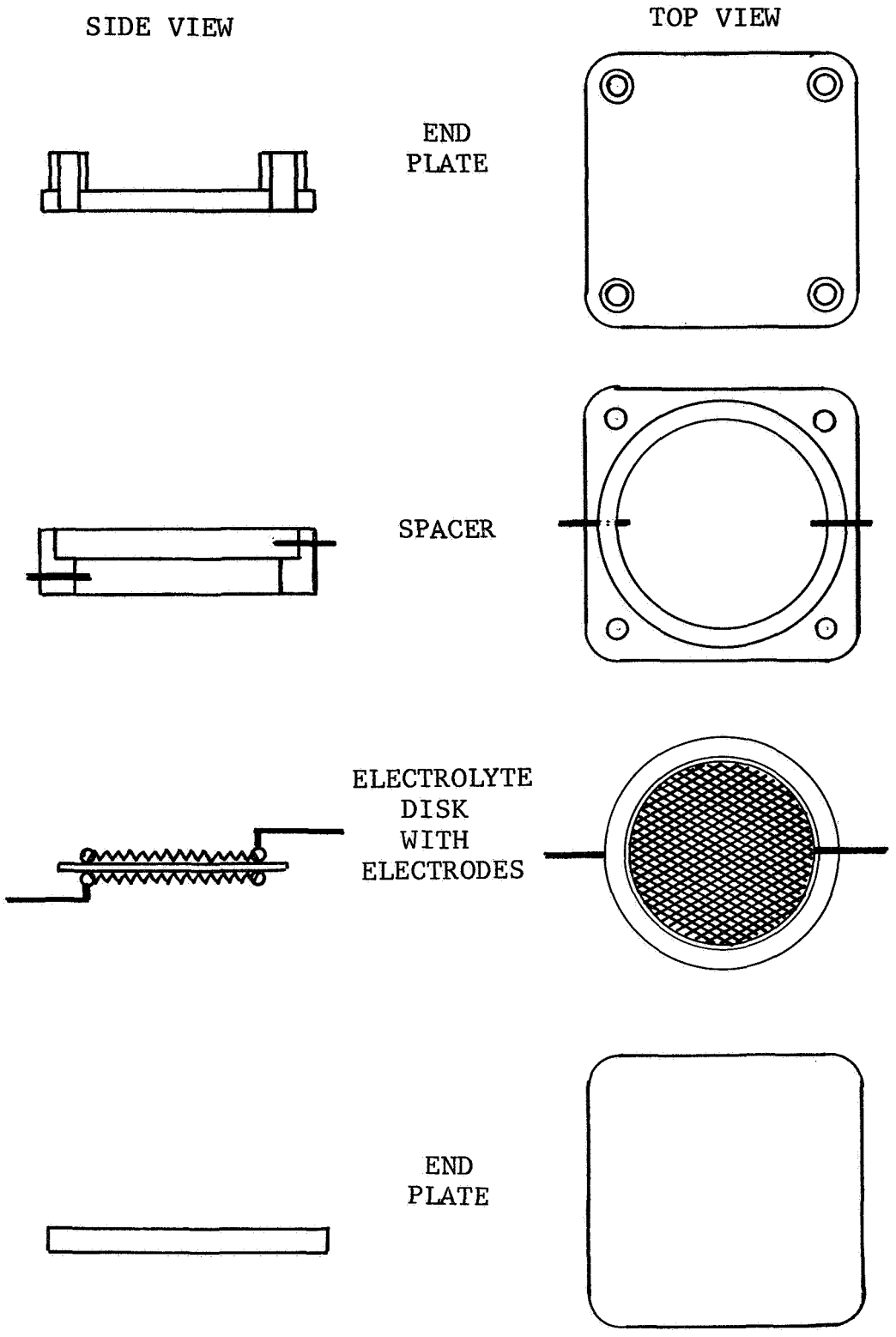

Fig. 2-3 Components of the Electrolyzer

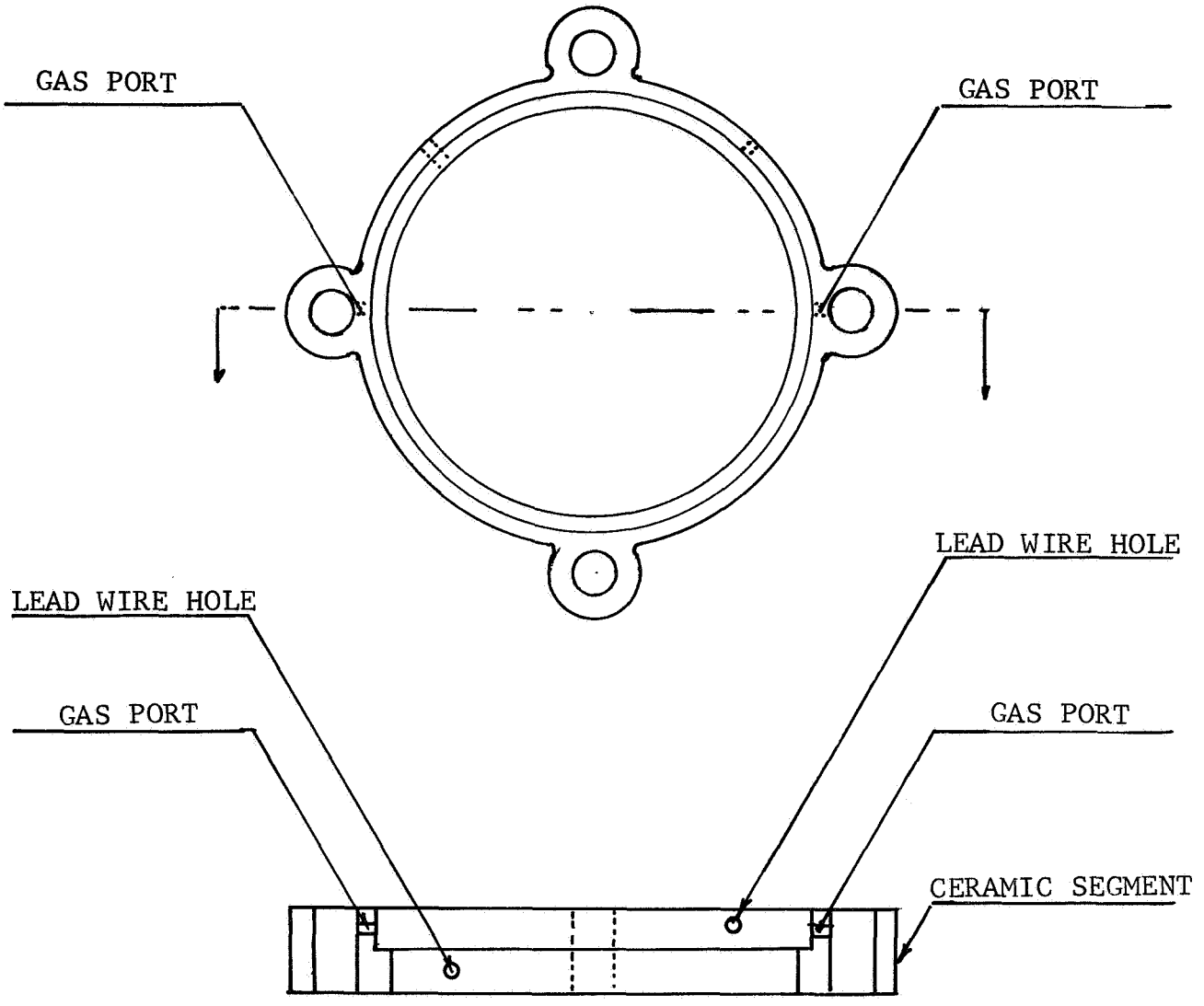

Fig. 2-4 Electrolyzer Design with Uniform, Thin Ceramic Walls

ing conditions of anode and cathode gas compositions, voltage and, probably, temperature. Each cell in a series flow arrangement would be operating on the exhaust gas from the cell ahead of it. Therefore, optimization of conditions in one cell implies operation of other cells under conditions removed from optimum. The parallel gas flow pattern of the design proposed above does not suffer from this defect.

2.2 TWELVE-AMPERE PROTOTYPE

For the 12-A CO_2-H_2O electrolyzer, the design using ceramic cell bodies and noble metal seals discussed in sub-section 2.1 and shown in Figs. 2-1 and 2-3 was chosen. This choice was based on the importance which we attach to the design principles discussed above and also on our having greater experience with ceramics than with fabrication techniques for high-temperature alloys. Thus, construction of the 12-A electrolyzer in this configuration utilizes many methods previously employed in the 1-A CO_2 electrolysis unit (Refs. 2 and 3). The designs of Fig. 2-4 above and Fig. 4-1 of Ref. 1, although they have more uniform wall thicknesses than the chosen version, were not considered for actual fabrication because of the very considerable practical difficulties that would be encountered in making these shapes in high-temperature refractory ceramics. We felt that the modification shown in Fig. 2-3, although it has relatively thick, non-uniform walls, could be made in numbers adequate to develop the technology of solid oxide electrolyte devices for life-support purposes in the time permitted by the program schedule. The design principles discussed in the preceding sub-section are incorporated in this design.

The 12-A electrolyzer was constructed as a stack of three disks, each having an electrode area of 20 cm^2 operating at a current density of 200 mA/cm^2, with gas chambers between them. This design is shown approximately full scale in Figs. 2-5 and 2-6. A single cell of the stack is shown in Fig. 2-7. All parts are ceramics except for the lead wires and electrodes, which are noble metals. Three 12-A units of this type were built and operated.

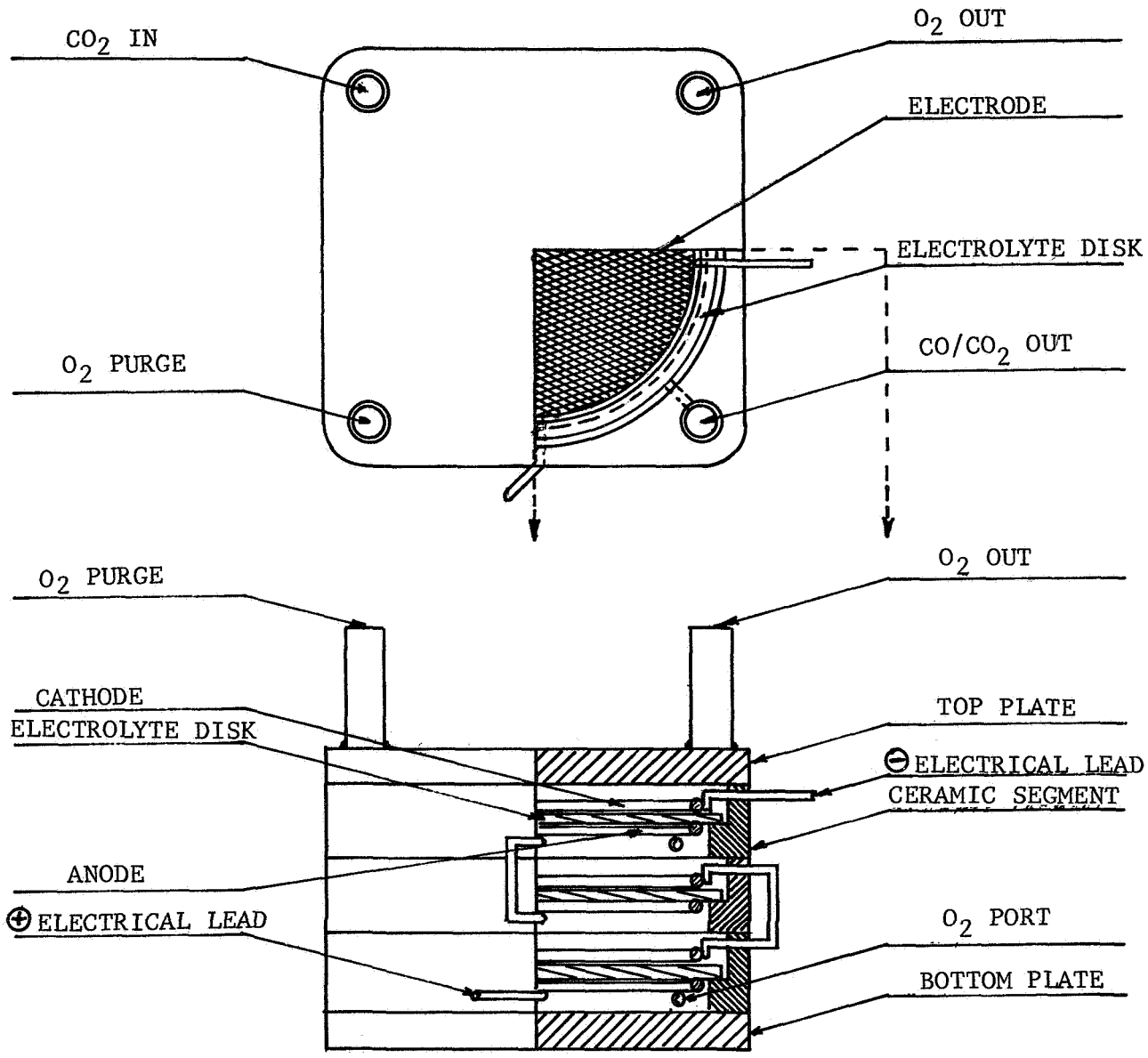

Fig. 2-5 Cutaway View of the 12-A Unit

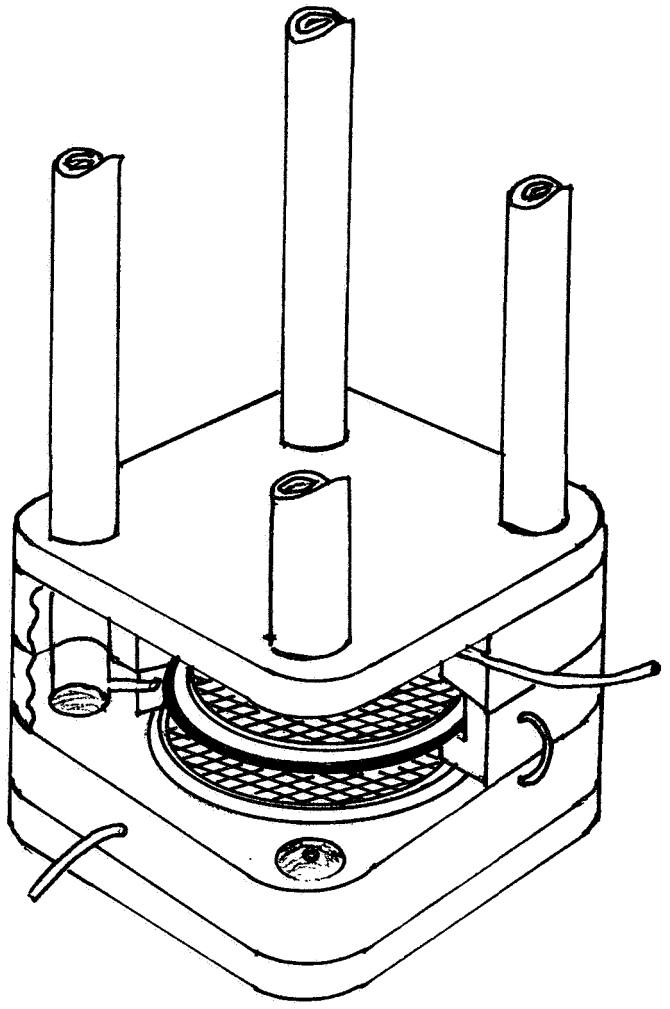

Fig. 2-6 Perspective View of the 12-A Unit

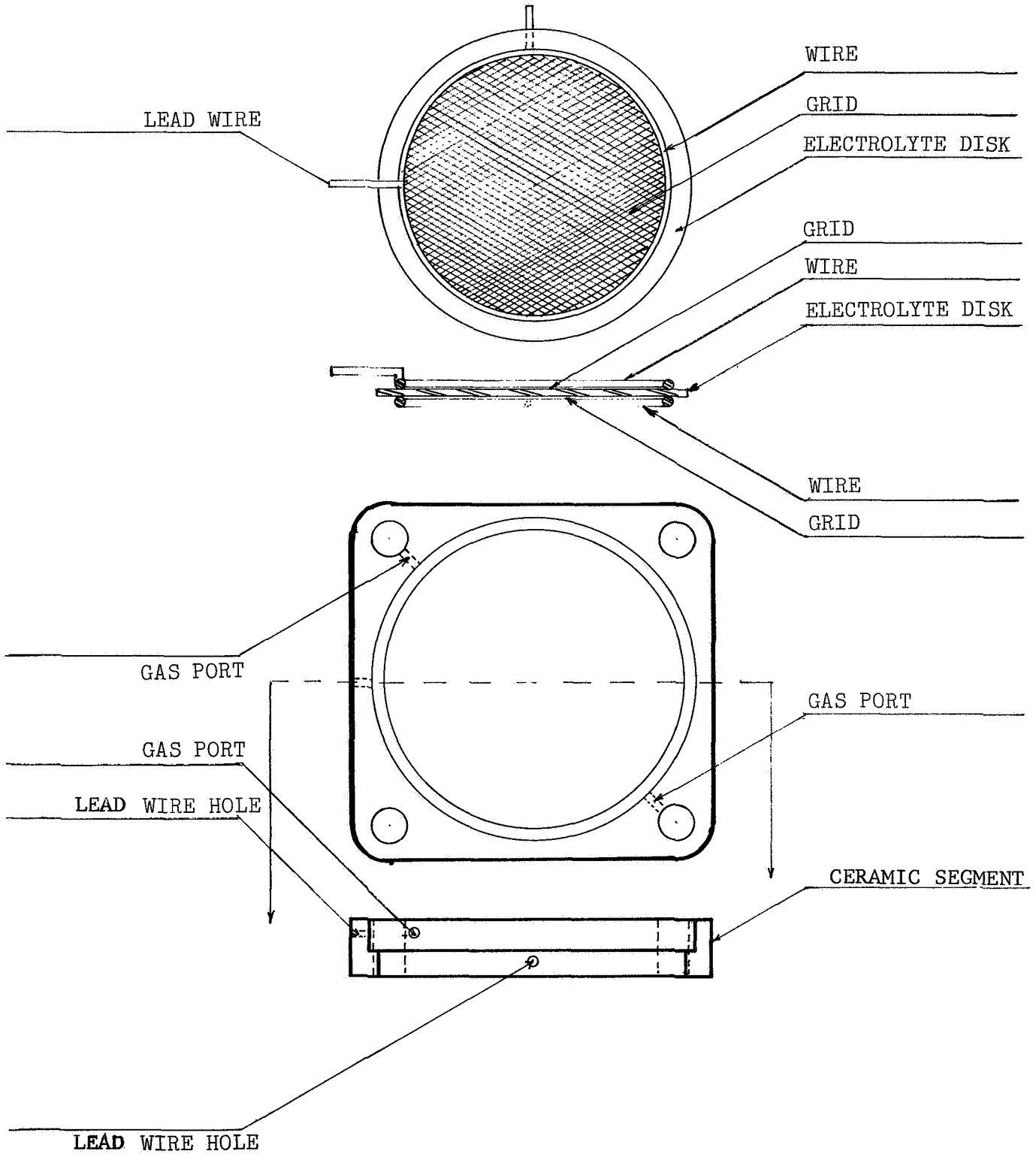

Fig. 2-7 Components of an Individual Cell

Section 3

FABRICATION OF THE TWELVE-AMPERE ELECTROLYZER

3.1 ELECTROLYTE DISKS

All the stages in the manufacture of electrolyte disks for the 12-ampere unit, powder preparation, densification by hot pressing, slicing and polishing, were performed in-house. Three types of powder, ZrO_2-CaO, ZrO_2-Y_2O_3 and ZrO_2-Sc_2O_3, were employed, all yielding hot-pressed compacts of high density, stabilized zirconia.

Hot pressing was carried out in a 45KVA, Astro Industries vacuum press. A schematic view of the essential parts is given in Fig. 3-1. Although the complete hot press was available, a great deal of effort was required for the assembly, repair and check-out of the sub-systems including the muffle furnace and press section, power supply, hydraulic, water-cooling, vacuum-pumping, and temperature-control systems. The operational details of only the furnace-press section will be discussed here.

All dies used were machined in-house from high-strength graphite stock, usually National, ATJ. The die body size was limited by the size of the furnace cavity to an o.d. of six inches and a height of nine inches. Hot pressings for electrolyte disks of the desired size require a nominal 2.5 inch die cavity, which leaves a die body wall thickness of 1.75 inches. This thickness has proved sufficient to contain the 4,000 psi internal die cavity pressure which could be generated by the ten-ton Astro press.

Various methods of die filling, pressing and heating sequence were investigated. By experience, a procedure was adopted that gave long die life and consistently good compacts with ZrO_2-Sc_2O_3 powders. The die was filled outside the furnace with bottom piston in place. Charges of approximately one pound of sub-micron size powder (as determined by microscopic examination and photomicrographs) were used. After insertion of the top piston, the charge was compressed on an auxiliary press, before setting up in the Astro furnace.

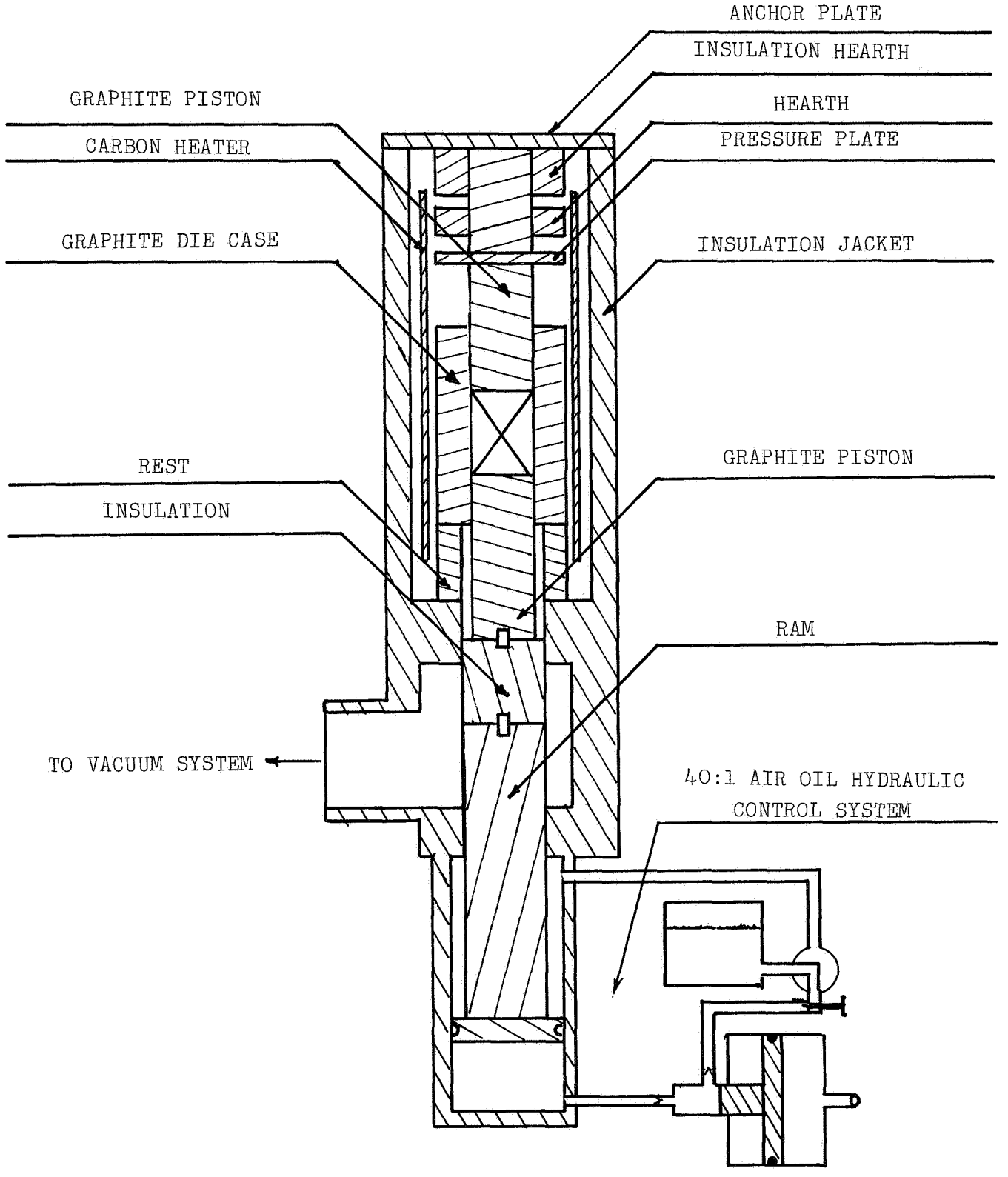

Fig. 3-1 Schematic View of the Hot Press and Muffle Tube Assembly (Scale: 2 Inches = 1 Foot)

After securing the furnace, the system was pumped down and vacuum tightness checked. Ram pressure was applied at room temperature and the furnace heated, initially at a slow rate until out-gassing had fallen off. The heating rate was then increased to about 20°C per minute. Up to about 1000°C, the powder and die increased in volume, and it was necessary to bleed oil from the hydraulic system to maintain the desired ram pressure. In the temperature range of about 1100 to 1400°C the volume shrinks due to rapid densification of the powder. During this stage the ram pressure was maintained automatically. Following each small reduction in pressure, the hydraulic amplifier was recharged with the emission of a "glugging" sound. For a given weight, powder type, and pressure, the number of "glugs" was constant. The absence of "glugs" signaled the end of rapid densification. Movement of the hot-pressing ram during densification of the oxide ceramic compact has been precisely followed by other workers using a linear variable differential transformer (LVDT) attached to the hydraulic plunger (Ref. 4). This device allows plots of ram displacement versus both temperature and time to be made as an aid to establishing optimum conditions of temperature and pressure for the particular powder being hot pressed. The Astro hot press did not lend itself to easy installation of an LVDT and counting the "glugs" was adopted as a qualitative substitute.

The rapid densification stage, which takes place by sliding, fragmentation and plastic flow of the powder particles was usually not sufficient to give a low porosity compact. The furnace temperature was raised beyond the final "glugging" value to allow further densification by a bulk diffusion process (Refs. 4, 5 and 6). During this period the ram pressure increased slowly. As the furnace temperature reached the final, pre-set value, the heating rate had fallen to about 10°C per minute. The final temperature was held automatically, and the die temperature checked with an optical pyrometer. After soaking at temperature, the ram pressure was relieved and the ram backed off. Following another soak period, the furnace temperature was reduced manually at a rate not exceeding 12°C per minute.

The details of the pressing runs made for electrolyte disk preparation are given in Tables 3-1 through 3-3. (In the case of the ZrO_2-CaO powder, the 2.48 inch round die runs were for electrolyte disks.) The powders are designated by

Table 3-1

HOT PRESSINGS - ZrO_2-CaO POWDER

Pressing	Type Die (inches)	Powder	Pressure (psi)	When Applied	Temp (°C)	HOLD PERIOD With Pressure	HOLD PERIOD Without Pressure	Sp. Gr.	% Theoretical ***
G-1	2.48 R*	B-8 (13.0%) VAR	2,100	at ≈950°C	1,407	none	-	4.51	83
G-6	2.48 R	B-3+7(14.0%) VAR	4,150	at RT	1,530	20 min.	-	5.50	100
G-7	2.48 R	B-4+9(13.0%) VAR	4,150	at RT	1,515	10 min.	-	5.46	100
G-12	2.75 S*	(10.0%) ZIRCOA B	2,070	at RT	1,520	26 min.	15 min.	5.24	91
G-14	-	(10.0%) ZIRCOA B	-	-	-	DIE BROKEN		-	-
G-22	square (with inserts)	(10.0%) ZIRCOA B	2,200	at 1025°C	1,595	22 min.	15 min.	5.23	91
G-33	2.75 S	(10.0%) ZIRCOA B	2,500	at RT	1,605	26 min.	10 min.	5.53	97
**G-42	2.48	(10.0%) ZIRCOA B	2,450	at RT	1,510	12 min.	10 min.	4.69	82

*R denotes round, S denotes square.

**Pressed in Argon atmosphere; other pressings in vacuum.

***Error in these specific gravities is estimated to be ±1%.

Table 3-2

HOT PRESSINGS - ZrO_2-Y_2O_3 POWDER

Pressing	Powder	Pressure (psi)	When Applied	Temp. (°C)	HOLD PERIOD With Pressure	HOLD PERIOD Without Pressure	Sp. Gr.	% Theoretical**
G-2	B-13 (9.4%) TAM	3,350	at RT	1400	20 min.	-	5.35	89
G-3	B-14 (9.4%) VAR	4,000	at RT	1520	20 min.	-	5.85	98
G-4	B-15 (9.4%) VAR	4,150	at RT	1530	9 min.	-	5.88	98
G-5	B-5 (10.2%) VAR	3,950	at RT	1470	9 min.	-	5.63	94
G-8	B-17 (9.9%) VAR	4,150	at RT	1530	20 min.	-	5.85	98
G-11	B-12 (9.4%) TAM	2,100	at 1525°	1525	14 min.	30 min.	4.74	80
G-18	B-24 (10.0%) TAM	-	-	-	BREAKAGE IN FURNACE		-	-
G-19	B-25 (10.0%) TAM	3,500	at 1090°	1530	20 min.	20 min.	5.30	89
G-20	B-26 (10.0%) TAM	4,050	at 1090°	1640	15 min.	15 min.	5.55	94
G-41	B-27 (9.0%) TAM	4,100	at RT	1565	12 min.	10 min.	5.45	92
*G-44	B-26 (10.0%) TAM	4,050	at RT	1520	10 min.	10 min.	5.50	93
G-53	B-38 (10.0%) TAM plus 2.0% Fe_2O_3	4,140	at RT	1500	11 min.	10 min.	5.76	97
G-55	B-40 (10.0%) TAM plus 1.0% Fe_2O_3	4,150	at RT	1505	10 min.	10 min.	5.80	98

*Pressed in Argon atmosphere; other pressings in vacuum.

**Error in these specific gravities is estimated to be ± 1%.

Table 3-3

HOT PRESSINGS - ZrO_2-Sc_2O_3 POWDER

Pressing	Powder	Pressure (psi)	When Applied	Temp. (°C)	HOLD PERIOD With Pressure	HOLD PERIOD Without Pressure	Sp. Gr.	% Theoretical*
G-9	B-18 (7.9%) VAR	4,150	at RT	1525	20 min.	10 min.	5.75	99
G-10	B-19 (8.0%) VAR	4,150	at 1500°	1500	20 min.	cool with stationary ram	5.74	99
G-13	B-20 (8.0%) TAM	3,460	at RT	1525	20 min.	20 min.	5.63	97
G-15	B-21 (8.0%) TAM	3,320	at RT	1650	6 min.	6 min.	5.59	96
G-16	B-22 (8.0%) VAR	3,560	at 1095°	1530	20 min.	20 min.	5.80	100 contaminated
G-17	B-23 (8.0%) TAM	-	-	-	Breakage in furnace		-	-
G-25	B-29 (8.0%) TAM	3,500	at RT	1600	10 min.	11 min.	5.60	96
G-31	B-32 (8.0%) TAM	3,950	at RT	1605	11 min.	10 min.	5.65	97
G-32	B-33 (8.0%) TAM	3,900	at RT	1605	11 min.	10 min.	5.65	97
G-47	B-34 (8.0%) TAM	3,540	at RT	1600	10 min.	10 min.	5.61	96
G-50	B-36 (8.0%) TAM	3,510	at RT	1565	10 min.	10 min.	5.56	95
G-51	B-34+36(8.0%)TAM	3,590	at RT	1565	12 min.	10 min.	5.56	95
G-54	B-39 (8.0%) TAM	3,560	at RT	1570	10 min.	10 min.	5.55	95
G-56	B-41 (8.0%) TAM	3,740	at RT	1525	12 min.	10 min.	5.55	95
G-57	B-39+41(8.0%)TAM	4,050	at RT	1520	10 min.	10 min.	5.57	96

*Error in these specific gravities is estimated to be ± 1%.

batch number, mole percent of CaO, Y_2O_3, or Sc_2O_3 in parenthesis, and source of zirconyl chloride in capitals. The designation VAR refers to high-purity material obtained from the Varlacoid Chemical Company, and TAM refers to a commercial grade obtained from the Tam Division of National Lead. The density of the hot-pressed compacts was determined by measurement of dimensions and by water displacement. The theoretical density was determined, for each powder type, by x-ray diffraction of powder specimens from the pressed compacts after air firing. In every case, the only lines observed on the diffractometer record were those of the desired cubic, stabilized zirconia.

To be useful as electrolyte disks, the thin slices cut from the pressed compacts must be relatively gas-tight. To achieve this condition using hot pressing in vacuum, we have found that the ceramic must have a significantly higher density than was necessary for the same degree of gas permeability in the case of the electrolyte disks prepared for the former lollipop cells by cold pressing and sintering. It would appear that, for zirconia, vacuum hot pressing leads to a greater degree of interconnection of pores than does cold pressing and sintering in air.

Compacts of ZrO_2-CaO having theoretical density were prepared (see G-6 and G-7 in Table 3-1) but they were full of cracks and, therefore, not useful for the preparation of electrolyte slices.

The hot-pressed ZrO_2-Y_2O_3 compacts did not exhibit the multiple, coarse cracks of the ZrO_2-CaO pressings, but suffered from a different defect, namely strain. To obtain leak-free slices, the ZrO_2-Y_2O_3 compacts had to have an average bulk density of at least 94% of the theoretical x-ray density. Several such pressings were obtained (see Table 3-2). In every case a strain was present which resulted in a splitting into two pieces. Those compacts which did not split on cooling in the die were processed into thin slices and fired in air to 1300°C. All slices so treated "flew apart" due to residual strain. Slices from the earlier, high-density ZrO_2-Y_2O_3 pressings (G-3 and G-4) were air fired to 1200°C. Some survived these conditions intact and then failed during the subsequent electrode application procedure. The 1300°C firing was adopted as a better test of residual strain. Several variations in hot-pressing conditions to produce a

strain-free ZrO_2-Y_2O_3 compact were tried without immediate success. G-44, pressed in an argon atmosphere to reduce interconnection of residual pores, gave relatively gas-tight slices which still failed by strain cracking. The Fe_2O_3 contents of the powders used in G-53 and G-55 gave very high densities for Tam material; however, an iron-rich, second phase was produced.

The use of ZrO_2-Sc_2O_3 powder has been quite successful for the preparation of electrolyte disks by vacuum hot pressing. All of the pressings listed in Table 3-3 (except G-10 and G-16) yielded disks which have survived the 1300°C air firing. (In G-10, the compact was cooled in the die with ram pressure applied, resulting in fracture due to excessive pressure at reduced temperature. In G-16, the powder batch was contaminated with a water soluble impurity which leached out on slicing. For the ZrO_2-Sc_2O_3 pressings, the major source of loss is mechanical breakage during the slicing and polishing operation.

A significant variation in density occurs within a given pressing as determined by leak checks on slices as a function of distance from top of pressings. The density increases (porosity decreases) from top to bottom of a given pressing. For a ZrO_2-Sc_2O_3 compact having a nominal bulk density below about 95%, roughly half the pressing is too porous for use as electrolyte material. The pressing becomes completely impermeable at a nominal value of about 99%. As the density increases, the pressings become very hard and difficult to slice, and the mechanical loss goes up. By experience, hot-pressed compacts were produced such that all slices were useable as electrolyte disks. The variation in density within a pressing is probably caused by the press design. In the Astro hot press the ram pressure is applied only to the bottom die piston. The use of a free-floating die body is apparently not sufficient to overcome the effect of pressing from only a single direction.

ZrO_2-Y_2O_3 and ZrO_2-Sc_2O_3 pressings were made using both Varlacoid and Tam source materials. The trend in the data indicates that a denser specimen is obtained with the higher purity Varlacoid for a given temperature-pressure profile; however, the readily available, commercial Tam material gives good disks, and its use results in a significant savings in the raw materials cost. After air firing, the Varlacoid disks are dead-white while the Tam disks have a

pronounced yellow color due to the impurities. Both types have the same oxygen conductivity, as a function of temperature, within experimental testing precision; and both types are translucent, as would be expected for high-density, cubic phase material.

For slicing, a cylindrical rod is glued to the face of the pressed compact. The rod is clamped in a movable vise on a diamond cut-off saw. After much experimentation with various types of diamond wheels and fixture geometry, it has been determined that a wheel imbedded with large diamonds gives the fastest slicing, longest life, and least breakage of disks. Apparently, a chipping action is superior to a grinding action for slicing this hot-pressed material. In operation, the vise is pulled toward the water-cooled saw blade by a weighted lever arm and pulley, taking about two hours for each slice. Depending on the thickness of the blade, about .127 to .190 cm of the pressing is lost for each slice. This is greater than the slice thickness.

Depending on the final disk thickness desired, the slices are cut slightly oversized and then lapped on diamond polishing wheels to give a disk with flat parallel faces. The polished disk thickness used during this period has been mainly in the range .063 to .127 cm. The disks are then vacuum leak checked, pickled briefly in acid, washed, dried, and then fired in air for about four hours at a nominal 1300°C. Over five dozen disks of ZrO_2-Sc_2O_3 have been prepared by this procedure. Most of the loss occurs in slicing (slices too thick, chipped edges and the like). None has been lost on air firing.

Due to the reducing conditions in the hot press and contact of the compact with the walls of the graphite die, surface carbiding and blackening can be noted across the face of the disks. This is seen in Fig. 3-2 as a function of penetration depth due to diffusion of oxygen radially outward during reduction. Several disks have been weighed before and after oxidation by air firing. The weight gain for ZrO_2-CaO samples (from pressings G-6 and G-7) varied from 0 to 100 parts per million. The ZrO_2-Sc_2O_3 (G-9) was intermediate, with weight gain values ranging from 80 to 350 ug/g. All of the weight gains listed above have been from pressings made with Varlacoid material. For Tam source material, the weight gain for ZrO_2-Sc_2O_3 samples (G-13 and G-15) was significantly higher, in the range of 650 to 1,000 parts per million, pre-

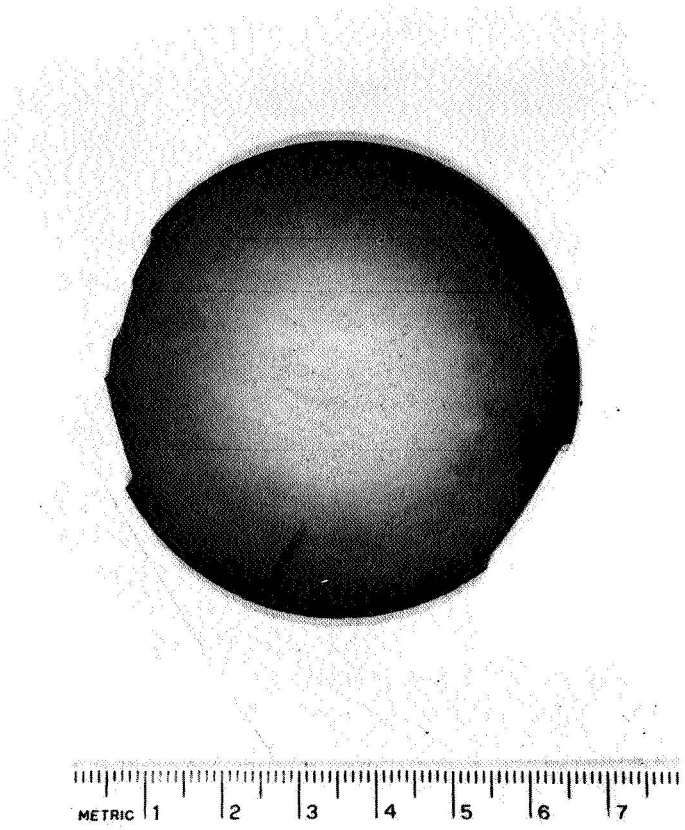

Fig. 3-2 Blackening of the Outer Rim of a Disk Due to Reduction in the Hot Press

sumably because of the presence of a reducible impurity, such as TiO_2.

The final step in the preparation of an electrolyte disk is the application of electrodes. The central area of the disk, which is to be covered with an electrode, is first painted with a thin coat of unfluxed platinum paste (currently using Engelhard-Hanovia #6926) and then fired in air for approximately two hours at a nominal 1200°C. A 5-cm circle is cut from .01 cm thick, expanded platinum mesh, and a .05 cm platinum wire is bonded to the circumference of the mesh by spot welding. A "tail" of the .05 cm Pt wire is left free for later connection of the electrode to the lead-through in the body segment. The air-fired first coat is repainted, the platinum mesh circle laid on, another coat is applied and the assembly is fired as before. Fig. 3-3 is a photograph showing the appearance of the finished disk with electrode in place. Electrodes are affixed to both sides of the disk at the same time.

3.2 CELL BODIES

Zirconia is the obvious choice for the body segments because of its close match in coefficient of thermal expansion with the disks and because of our previous successful sealing experience with zirconia-to-zirconia seals in the lollipop units. Accordingly, a great deal of effort was expended in diamond sawing, core drilling, and grinding high-density zirconia plates of commercially available compositions purchased from a vendor. Out of a total of thirty plates, several had visible external cracks or striations and were not processed and most of the rest had internal cracks, striations, or large voids which were apparent after various stages of the diamond machining operations. These faults forced all but seven bodies and five end plates to be rejected. Because of the high rejection rate, wear on the diamond tools has been very severe, being appropriate not to seven bodies but to several times that number. The procedure described below for cell body fabrication was evolved from experience gained during the operation. All work was performed in-house.

As-received, round plates are visually inspected and those with obvious flaws rejected. The balance are air fired at a nominal 1300°C to detect strained pieces which fly apart under thermal cycling. The surviving plates are then squared-

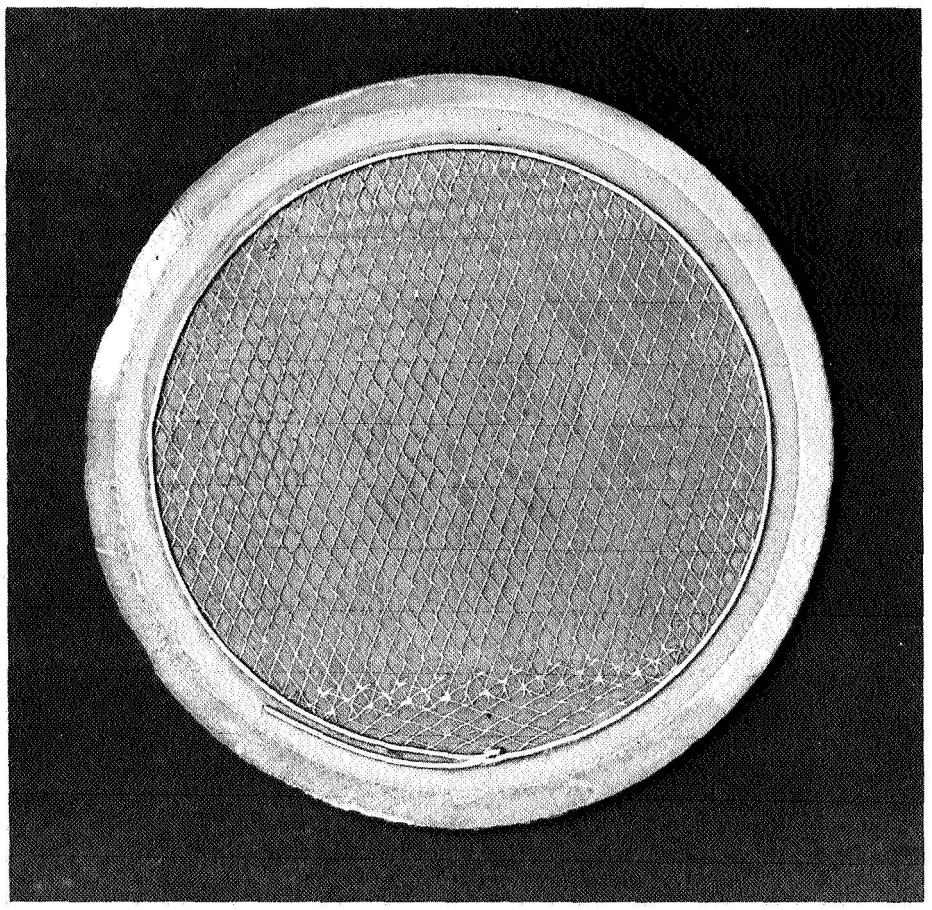

Fig. 3-3 Electrolyte Disk Showing Electrodes and Sealing Rim

off on the diamond cut-off saw described in 3.1. The 7.0 cm square plates are mounted in a holding jig fastened to the table of a water-cooled drill press for ceramics. The 5.85 cm center hole is cut first using a diamond core drill. If no large internal flaws are found, the piece is counter-bored to form the sealing ledge using a 6.35 cm diameter diamond core drill. The corner edges are rounded off on a diamond lapping wheel. The piece is then mounted in an oscillating drill press where the .10 cm gas ports and electrical lead-through holes are drilled using a solid diamond drill. The body is again air fired at a nominal 1300°C to allow it to warp, if so inclined. The last step is to lap the opposite faces flat and parallel and buff the sealing ledge prior to the electroplating operations to follow. A photograph of a finished cell body component is shown in Fig. 3-4.

Several attempts were made to hot press zirconia body blanks. Since the square bodies have a total area over one and a half times greater than the electrolyte disks, the effective die pressure of the Astro hot press is limited to about 2500 psi. The first square die was made by milling a 7.0 cm square hole (with rounded corners) in a graphite cylinder with matching pistons. The fit between pistons and die cavity, of necessity, could not be as close and as uniform as for a cylindrical die. This die lasted for only one run. On the second run, the die fractured and broke the graphite heater of the hot press. Subsequent square dies which could be employed for several hot pressings were constructed using a novel technique. Graphite shim-plates were made, so that when placed around the circumference of the square pistons, a cylinder was produced that could be fitted closely to the i.d. of a cylindrical cavity. Since the o.d. of the die body is limited to six inches, the die wall thickness is reduced to about 1.6 inches. This has been found sufficient to contain an internal cavity pressure of 2500 psi.

A commercially available, stabilized zirconia powder, Zircoa B (10 mole% CaO in ZrO_2) was employed for hot pressing cell bodies (see Table 3-1). The average 91% density pressing obtained in G-12 had a low enough permeability at the bottom, but was too permeable at the top. Increasing the temperature and pressure to the conditions of G-33 gave a 97% dense compact which had low permeability throughout. However, the G-33 pressing was strained and fractured on air firing just like the high-density ZrO_2-Y_2O_3 compacts. In run G-42, the

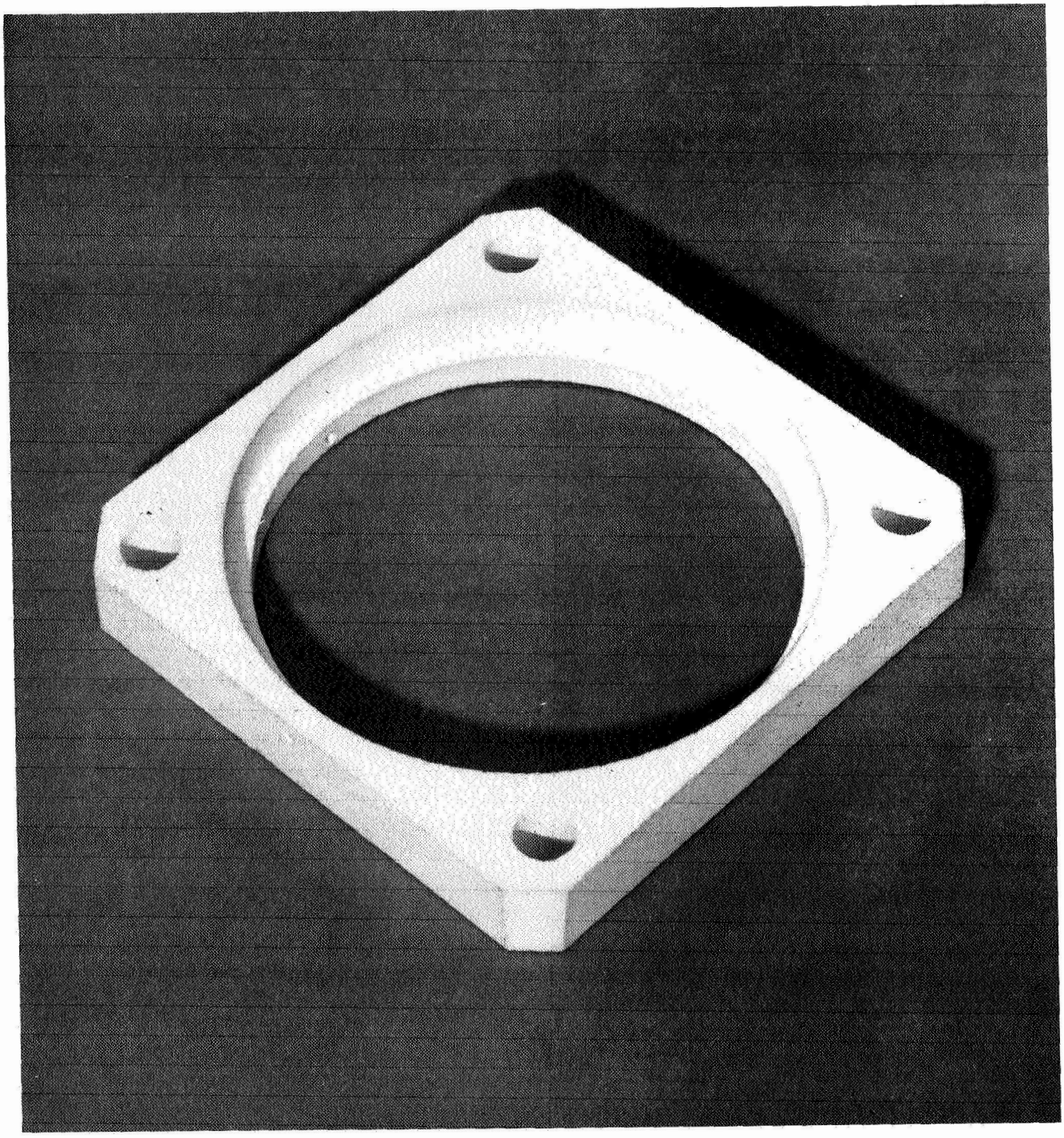

Fig. 3-4 Ceramic Cell Body

pressing was carried out in an atmosphere of argon, instead of the usual vacuum. It was hoped that this might lead to less channelization of pores and thereby a reduced permeability. The result was a net increase in porosity due to a much lower achievable density. In G-22, the square die assembly was fitted with a central, hollow graphite core to produce a cell body with pre-formed center hole. The pressing cracked on cooling due to the differential shrinkage between the ceramic body and the graphite core.

A high degree of success has been achieved in hot pressing cell body components from magnesium oxide (see Table 3-4). Commercially available, USP grade MgO is used without further treatment. The higher bulk density "Heavy-Grade" powder appears to hot press better than the "Light" powder, and requires no pre-compaction to get enough powder into the die for a full-thickness cell body component. Among the MgO pressings produced only two have fractured on subsequent air firing (which is carried out at a nominal 1250°C to avoid approaching the hot-pressing temperature). These two pieces were full area end plates, which appear to be more sensitive to thermal shock than the center-core-drilled body segments. The body segments were shaped using the same diamond tooling described for ZrO_2. The MgO blanks were easier to machine, gave less tool wear, and did not fracture on machining. Eight cell body components and three end plates were produced.

A material of potential interest for the preparation of cell body components is fired talc (magnesium silicate), because its coefficient of thermal expansion is close to that of stabilized zirconia. The natural mineral is available as American Lava Corp., Lava grade 1136. A problem in using the natural stone is that only a fraction of the pieces are crack free and therefore suitable for fabrication of cell body components. A selection was made from a shipment of Lava 1136 plates, and a few found free enough of large-scale cracks to allow machining and firing into cell body components suitable for subsequent sealing tests.

Talc has the nominal composition $3MgO \cdot 4SiO_2 \cdot H_2O$, and, on firing at ~1100°C, loses water to become a steatite-like ceramic. The results of hot pressing talc are given in Table 3-5. In G-21, the product (probably not dehydrated) was full of cracks. For the remaining runs, USP grade talc was first dehydrated, as a powder, at a nominal 1100°C, to allow hot

Table 3-4

HOT PRESSINGS - MgO POWDER

Pressing	Powder	Type Die (inches)	Pressure (psi)	Temp. (°C)	HOLD PERIOD With Pressure	HOLD PERIOD Without Pressure	Sp. Gr.	% Theoretical ***
G-23	Light	2.48 R*	1,900	1,375	11 min.	12 min.	3.45	97
G-27	Light (Prepressed Pellets)	2.75 S*	2,060	1,375	11 min.	10 min.	3.47	97
G-28	Heavy	2.75 S	2,120	1,335	10 min.	10 min.	3.58	100
G-29	Heavy	2.75 S	2,120	1,335	10 min.	10 min.	3.58	100
G-30	Heavy	2.75 S	2,110	1,335	10 min.	10 min.	3.58	100
G-34	Heavy	2.75 S	2,080	1,325	10 min.	10 min.	3.58	100
G-35	Heavy	2.75 S	2,080	1,315	10 min.	10 min.	3.56	100
G-36	Heavy	2.75 S	2,080	1,315	10 min.	10 min.	3.56	100
G-37	Heavy	2.75 S	2,100	1,315	11 min.	9 min.	3.57	100
G-38	Heavy	2.75 S	2,070	1,315	10 min.	10 min.	3.55	99
G-39	Heavy	2.75 S	2,100	1,315	10 min.	10 min.	3.55	99
G-43	Heavy	3.53 R	1,980	1,320	11 min.	10 min.	3.54	99
**G-46	Heavy	3.53 R	1,970	1,350	10 min.	10 min.	3.41	96
G-48	Heavy	3.53 R	1,990	1,350	10 min.	10 min.	3.53	99

*R denotes round, S denotes square.

**Powder charge pre-pumped overnight prior to hot pressing.

***Error in these specific gravities is estimated to be ± 1%.

Table 3-5

HOT PRESSINGS - MAGNESIUM SILICATES

Pressing	Powder	Type Die (inches)	Pressure (psi)	Temp. (°C)	HOLD PERIOD With Pressure	HOLD PERIOD Without Pressure	Sp. Gr.	Remarks
G-21	Ground Lava 1136	2.48 Round	2,950	1,000	Slow approach to temperature		ave=2.41	Probably not dehydrated
G-24	B-31 Calcined Talc	2.48 Round	1,900	1,425	14 min.	10 min.	ave=2.52	-
G-26	B-31 Calcined Talc	2.48 Round	2,500	1,485	37 min.	11 min.	ave=2.45	Bottom white, end had density of 3.00
G-40	B-35 Calcined Talc	2.75 Square	2,510	1,515	41 min.	10 min.	2.86	In unmelted residue
G-58	B-35 Calcined Talc	2.48 Round	3,460	1,480	20 min.	10 min.	2.94	Bottom stuck to piston
G-59	B-35 Calcined Talc	2.51 Round	3,480	1,395	12 min.	10 min.	2.92	Good pressing
G-61	B-42 Calcined Talc	2.51 Round	3,480	1,370	12 min.	10 min.	2.88	Good pressing

pressing to higher temperatures. At test pressures of about 2500 psi (the maximum available for a full-area, square die) the compacts were too porous. Raising the pressure to nearly 3500, and dropping the temperature slightly, allowed the preparation of high quality pressings in the smaller, round die. To obtain the higher pressure in the larger cavity, square die, a center insert was employed. The high pressure, however, was too much for the thinner outer die wall.

Another magnesium silicate composition which has a coefficient of expansion close to that of stabilized ZrO_2 is synthetic forsterite, $2MgO \cdot SiO_2$. Several attempts to hot press a mixture of $MgO+SiO_2$ (under the conditions employed for calcined talc) gave porous compacts having 89% theoretical density.

A six-cell body, assembly mock-up was prepared from Lava A, a machinable, largely aluminum silicate stone available from American Lava Corp. This material is largely crack free and fires exactly to size; however, its expansion coefficient is too much smaller than stabilized ZrO_2 to allow sealing to electrolyte disks.

3.3 SEALING

3.3.1 Individual Cells

The noble metal sealing technique that proved reliable in the 2016-hr run of the lollipop unit was chosen as the basis for the seals in the 12-A unit. The large scale-up factor in both size and number of seals between the lollipop and the 12-A unit necessitated several modifications and extensions of this sealing procedure as follows:

(1) Whereas the lollipops contained two types of seals, namely, "conical" (or tube-to-body) and "ledge" (or disk-to-body) seals, the 12-A electrolyzer of the design described in sub-section 2.2 above requires four types of seals, namely, conical, ledge, body-to-body, and wire (electrical leads through the walls of the ceramic bodies) seals.

(2) Noble metal brazes melting at several temperatures were used to permit sealing the electrolyzer in stages rather than making all the seals simultaneously as had been done with the lollipop.

(3) Development work was carried out to extend the sealing technique to ceramics other than zirconia.

The basic sealing procedure for all four types of seals listed above was the same as that used in the lollipop (Ref. 3), that is, cleaning, sensitizing, and plating followed by furnace brazing in air with noble metal brazes. A series of experiments was conducted in which ZrO_2-Sc_2O_3 disks of approximately 6.35 cm diameter with thicknesses ranging from .063 to .14 cm were sealed into zirconia bodies. The rate of fracture of disks with thicknesses less than .10 cm was excessive leading to the adoption of the range .10 to .13 cm as our "standard" thickness for subsequent preparation of cells intended for the 12-A electrolyzer. The small number of good zirconia bodies available (see sub-section 3.2 above) necessitated removal of broken or unsealed disks after many of the experiments and re-plating of both disks and bodies. Our masking techniques were adequate to permit complete or partial re-plating as required without damage to the electrodes or to remaining plated areas.

Seals were made at temperatures above the gold point by the use of gold alloys instead of pure gold in the furnace brazing step of the sealing procedure. Changing from a pure metal to an alloy solid solution introduces the complication that each alloy has a melting range approximately equal to the temperature difference between the solidus and the liquidus of the appropriate phase diagram, rather than a sharp melting point. The exact melting range during a particular sealing operation depends on the rate of rise of the furnace temperature, the alloy composition, the nature of the sensitized surfaces, the relative amounts of fusible alloy and plated metal, and the geometry of the parts being sealed together. The furnace temperature-time profile and the geometry determine the temperature at the seal itself, a rise of this temperature above the solidus initiating melting. As an alloy melts, the composition of the liquid phase is different from that of the solid phase and the rate of melting will influence the extent of this disparity at any given time. The composition is further changed as the liquid metal wets and dissolves solid metal plated onto the ceramic surface being sealed. The nature of these surfaces (e.g., composition, density, roughness, porosity) and the ratio of fusible to non-fusible metal

both greatly influence the melting range and concentration gradients. At one extreme, the sealing alloy could fail to fuse adequately leaving an unsealed area and at the other extreme, the liquid metal could completely dissolve the plated metal coating from the ceramic leaving a gap.

Use of this sealing technique in practice depends upon a realization of the properties of alloys and melting conditions just discussed but it also relies on previous experience with the gold seals of the lollipop units and on observation of the results of empirical alloy sealing experiments. Gold-platinum and gold-palladium alloys melting over the temperature range 1085 to 1160°C were used. Measurement and control of the furnace temperature-time profile and visual observation of the sealing region and surrounding ceramic during a sealing run enabled the alloy technique to be used successfully. Top and bottom views of a sealed zirconia cell are shown in Figs. 3-5 and 3-6. The alloy bead can be seen around the perimeter of the electrolyte disk and on both electrical leads. The top and bottom surfaces of the segment are plated and are ready for sealing into the 12-A unit with lower melting alloys or gold.

Ledge seals (disk-to-body) of the type illustrated were sensitive to thermal shock and became leaky on cycling to 1000°C where the heat-up time was two hours or less. In subsequent assembly of three such cells into a 12-A unit (see the following sub-section), therefore, the rate of temperature change was carefully held to less than 2°C per minute. The wire seals exhibited no such tendency to leak.

In sealing experiments with ceramic bodies other than zirconia, the zirconia electrolyte disks were sensitized and platinum plated as before; the non-zirconia (e.g., magnesia) bodies and end plates were plated with metals matching their coefficients of thermal expansion and the brazed seal was made with alloys similar to those used in the zirconia-to-zirconia seals described above. The electrical leads were of a higher melting alloy than any to be melted in the sealing operations and matched the thermal expansion of the ceramic through which they were sealed. Approximate values of coefficients of thermal expansion for some materials of interest in this program are given in Table 3-6.

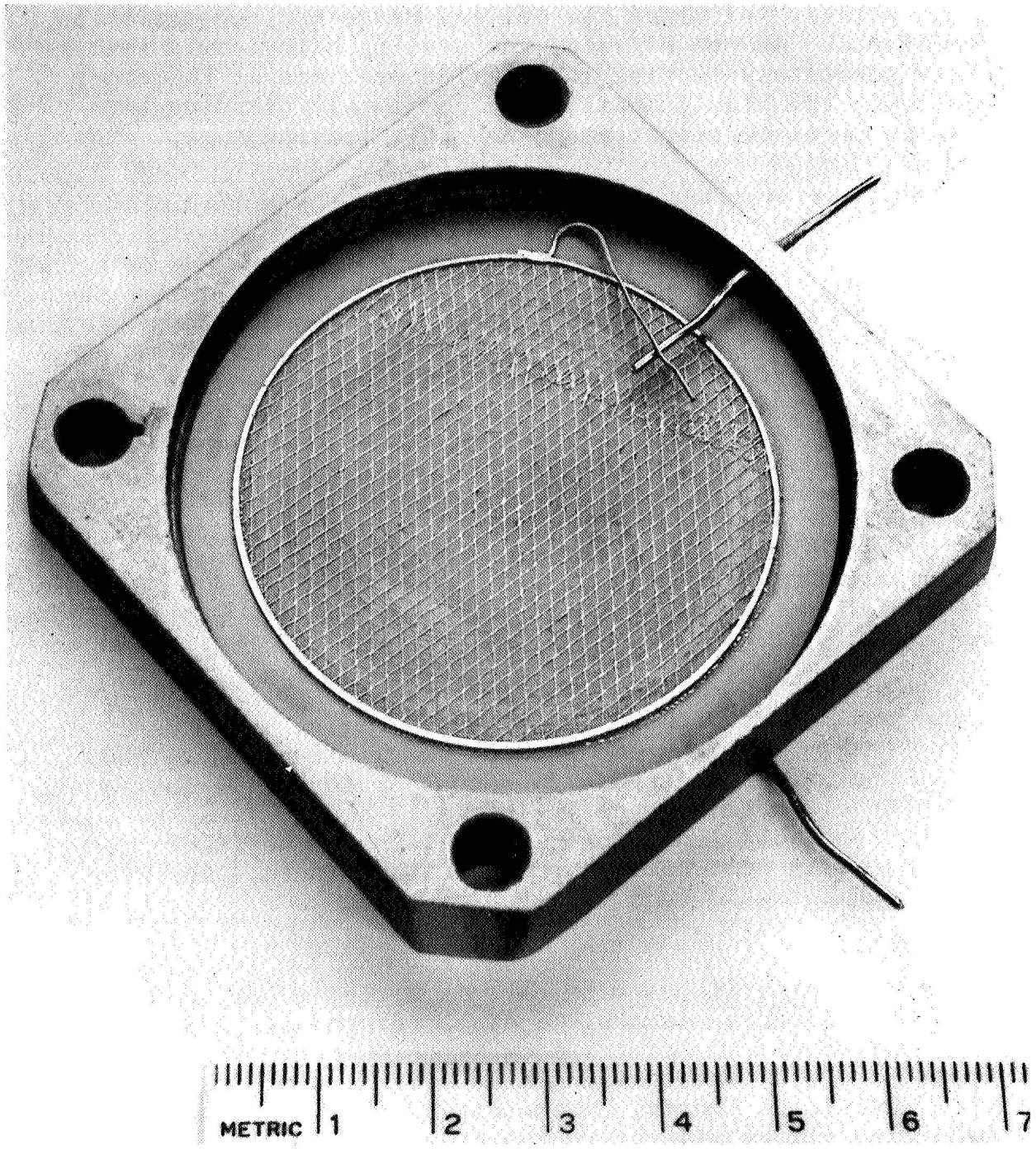

Fig. 3-5 Top View of a Zirconia Cell

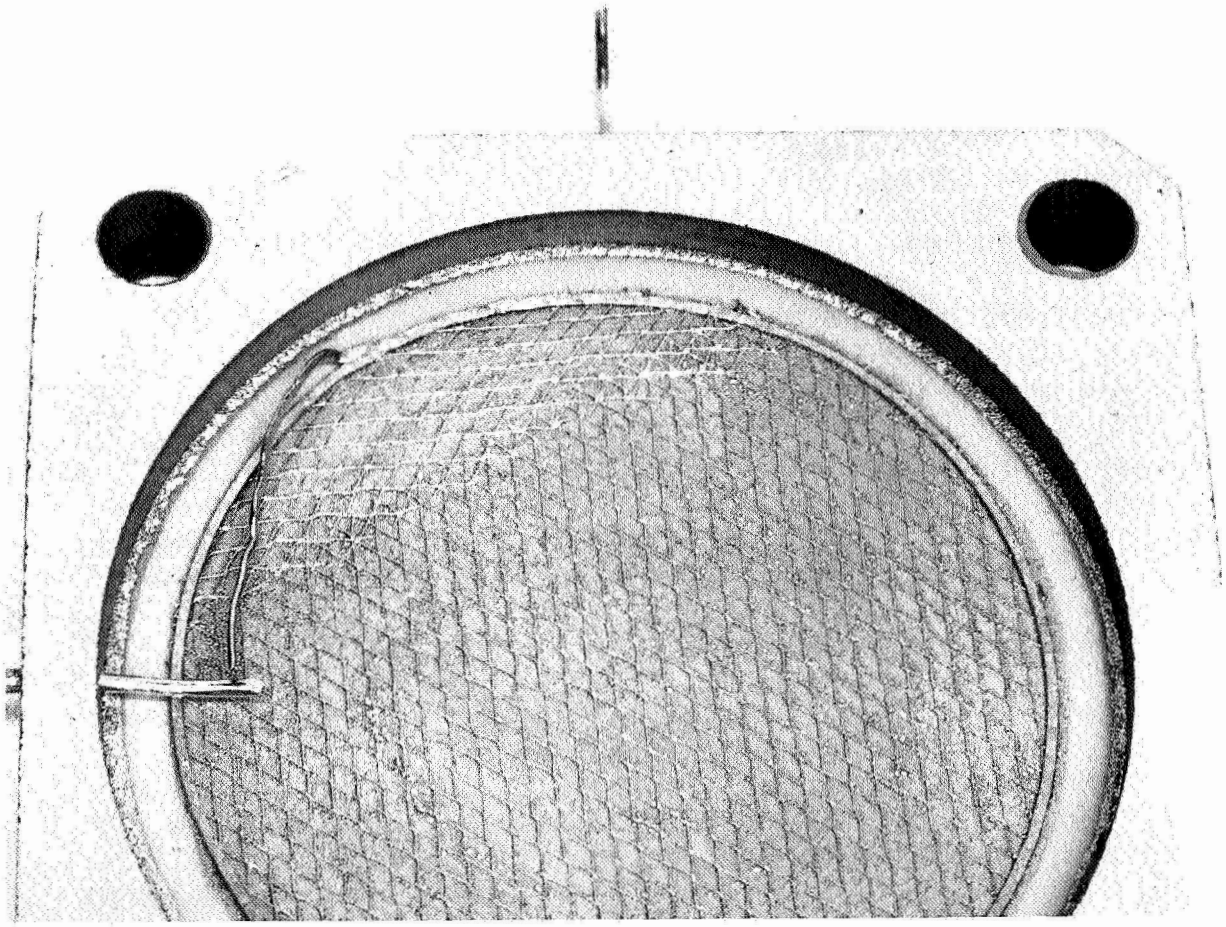

Fig. 3-6 Bottom View of a Zirconia Cell

Table 3-6

COEFFICIENTS OF THERMAL EXPANSION (10^7cm/cm-^oC)

Ceramics			Noble Metals	
MgO	160		Au	160
Lava 1136	110		Pd	130
ZrO_2	100		Pt	100
Al_2O_3	80		Rh	95
Lava A	40		Ir	75

It is apparent from Table 3-6 that the pure noble metals or suitable binary alloys can be used to match all of the ceramics except Lava A. For magnesia, the surface to be sealed was plated with a gold-palladium alloy having a melting range above that of the fusible alloys used to make the seal. Although, with magnesia bodies, no successful ledge seals were made, the wire seals were gas-tight. Successful gas-tight seals of both types were made with Lava 1136 bodies.

3.3.2 Multi-Cell Units

Individual cells, each consisting of a zirconia disk sealed into a ceramic body also carrying sealed-in .10 cm electrical leads as described and shown above, were sealed together in an additional furnace brazing operation using a lower melting alloy than that used to seal the disk and wires. Experimental body-to-body seals were made with both Lava 1136 and zirconia, three bodies in each case, before proceeding to assemble a 12-A electrolyzer. This sealing geometry presented no particular difficulties and gave very tight seals unaffected by cycling to 1000^oC.

The four zirconia gas manifold tubes were attached to the top plate by drilling conical holes in the plate, making conical ends on the tubes ground to fit, plating both surfaces, and brazing with gold-palladium alloy in the 1150^oC range. These seals also presented no difficulty and, although some minor leaks occurred in the first sealing run, they were easily resealed by adding additional gold prior to the body-to-body brazing operation. Later conical seals were

gas-tight as a result of the alloy braze alone, but gold was added as a precaution.

Using the techniques described above, a total of three 12-A CO_2-H_2O electrolyzers, each containing three 20 cm^2 cells, was built. Each unit used zirconia-calcia bodies and tubes. Two views of one of the 12-A units are shown in Figs. 3-7 and 3-8. No particular care was taken with the first two units as far as controlling the rates of temperature change during the final sealing operation and subsequent testing. Both units proved to have significant leaks between the cathode and anode chambers, although there were no external leaks. The assumption was made that the ledge seals (disk-to-body) had opened up slightly because of thermal shock and the two units were disassembled by melting the seals. No cracks were found in the disks, further strengthening the belief that the leaks were through the ledge seals.

Fabrication of the third 12-A electrolyzer followed the same procedure as the first two with two important modifications. Each of the three cells was leak-checked at a pressure of 0.5 psi using soap solution. Previous leak-testing was not done under controlled pressure. This test pressure applies a force of 2.5 pounds to the 5 square inch disk. When it is considered that the maximum pressure drop in the electrolyzer during its operation is of the order of 0.02 psi, a test pressure of 0.5 psi would appear to provide an adequate leak check. Apart from the quantitative pressure test, the other modification in assembly of the third unit was to control the rate of temperature change to less than 2°C per minute during final sealing and subsequent heat-up for testing. These assembly procedures yielded the 12-A electrolyzer for which testing and operational data are presented in Section 5 below.

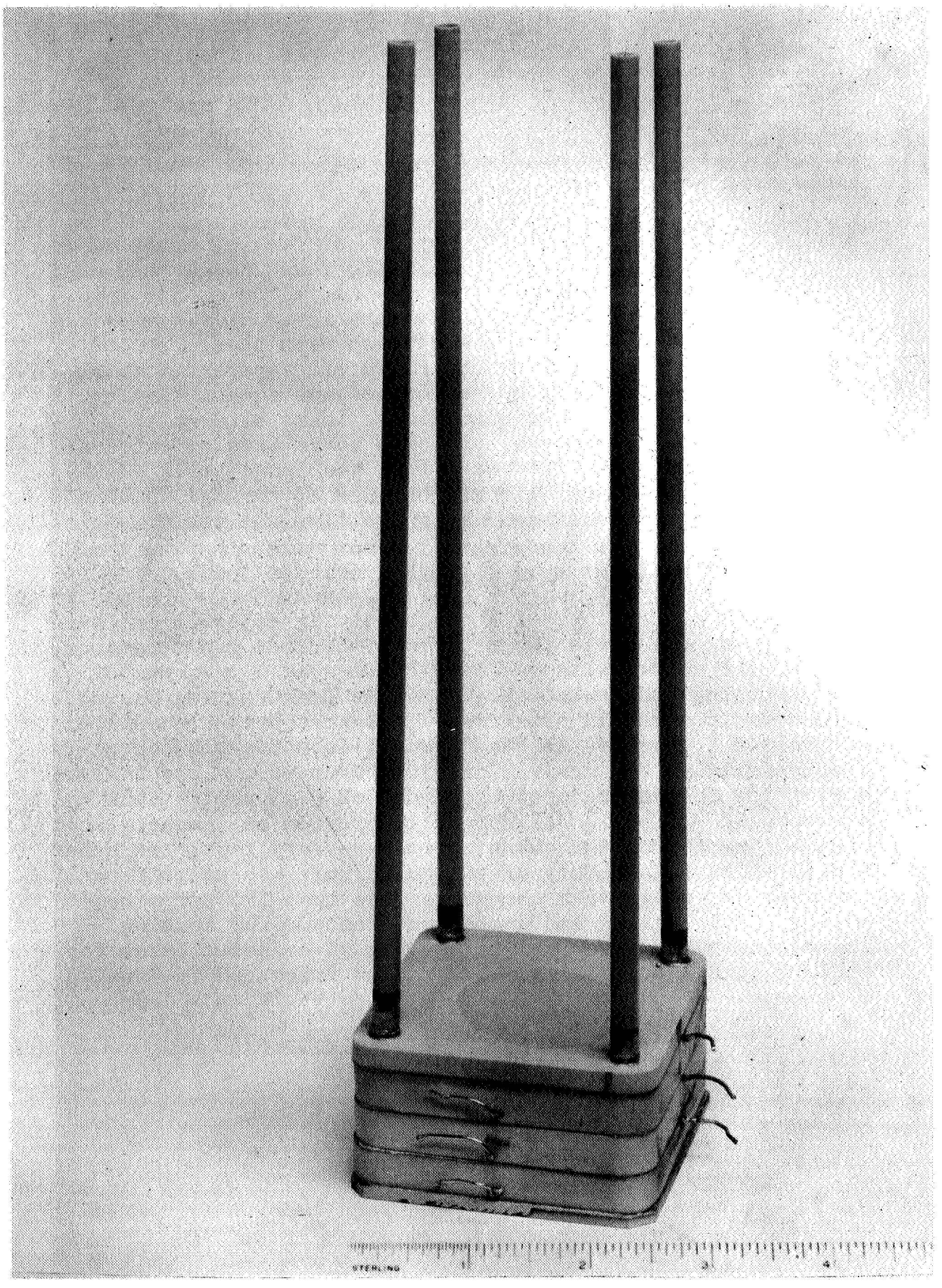

Fig. 3-7 Twelve-Ampere Electrolyzer

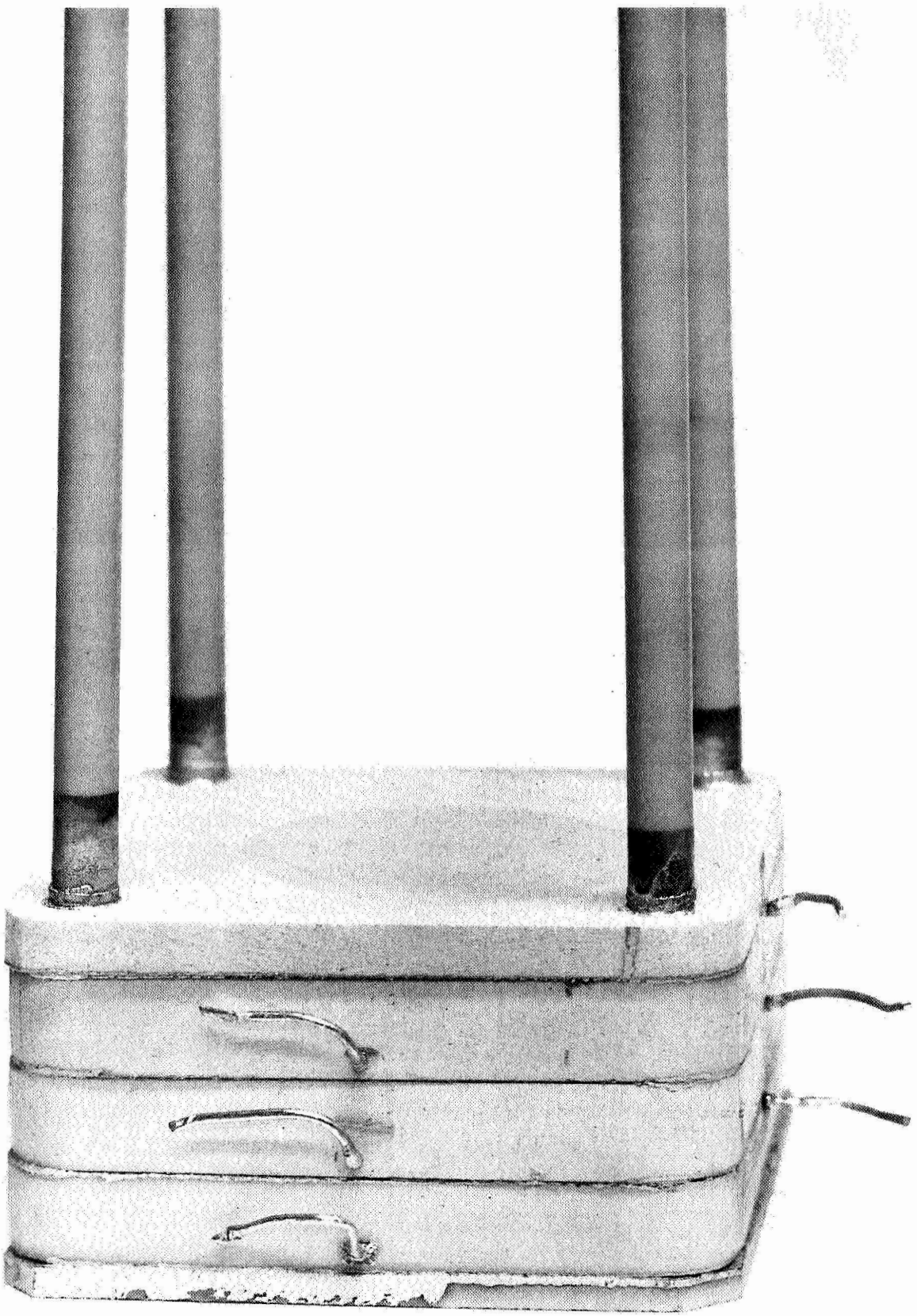

Fig. 3-8 Close-Up of Twelve-Ampere Electrolyzer

Section 4

CATALYTIC REACTOR

The catalytic disproportionation of carbon monoxide has been reported utilizing carbonyl iron (Ref. 7), Girdler catalyst H219 (NiO) (Ref. 8), and iron (Ref. 9) or steel. It seemed reasonable in our investigation to test the relative merits of such catalysts which in turn would aid us in designing a suitable reactor for the twelve-ampere carbon dioxide electrolyzer.

The investigation encompassed two main areas of endeavor: the design of suitable reactors and the test of several catalysts. Since it is well established that metals such as steel are good catalysts for carbon deposition, a mullite reaction vessel which is found to be non-catalytic was used to avoid the contribution of wall reactions.

The reaction vessel consisted of a mullite tube (30 mm i.d. and 450 mm in length) with suitable O-ring tapered joints. The catalyst was placed in the reactor and flushed with helium at the reaction temperature. The metered reaction gases (pure CO or a mixture of CO-CO_2 diluted with a few percent of hydrogen) were allowed to flow through the reactor which was vented to the atmosphere. At suitable time intervals, an aliquot of the effluent gas was diverted into the gas chromatography instrument and the reaction products were analyzed. A 10-H Poropak Q column and 2-ft. molecular sieve 5A column were employed at 35°C to separate the individual gas components. The flow rates of gases were measured employing calibrated rotameters. The reaction temperature was 575°C and the flow rate of reactant gas was 180 ml/min throughout this phase of our investigation.

Several test runs were made using carbonyl iron powder (General Aniline and Film Company, grade E). Whether carbonyl iron powder was dispersed on quartz wool (0.12 g catalyst) or placed in a combustion boat (0.54 g catalyst), about 10% of the initial carbon monoxide (initial $CO/CO_2=1$) was converted to carbon dioxide. After the run with a 50-50 mixture of CO-CO_2 was completed (carbonyl iron in boat), the

gas mixture was replaced with pure CO and tested. About 50% conversion was observed.

The catalytic efficiency of steel wool (2.5 g of 000 grade) was studied using carbon monoxide. The activity of the steel wool was increased with exposure to CO and reached a maximum rate after three hours. The maximum rate of conversion of CO was about 70%.

In view of the high catalytic activity of steel, a steel reactor was fabricated in which the wall of the vessel acted as the source of catalyst for the disproportionation of CO. A steel pipe (3 inches i.d.) was cut to desired length and a cap with a gas outlet port was welded on to one end. An O-ring flange with a gas inlet port was incorporated at the other end. The reactor was heated in a 12-inch long furnace.

After continuous operation for more than 40 hr, the reactor was cooled down and examined. The carbon had deposited along the hot zone of the wall over a distance of six inches and extended to a thickness of about an inch. The contents of the reactor were removed and found to weigh 87 grams. As shown in Fig. 4-1, the conversion rate of CO to CO_2 increased with exposure time and reached a maximum level of 75%. Using this reactor, a longer duration run was made with ~98% CO + ~2% H_2 to determine the maximum operating time that could be used before plugging would become a problem. The run was terminated after eight days (200 hr) of operation at which time there was no evidence of plugging (no pressure rise in the reactor). Upon examination of the reactor, the entire cross-section of the pipe was filled with carbon deposit. It is of interest to note that a reactor pre-conditioned by previous use as a CO disproportionator exhibited no induction time (Fig. 4-1, 2nd Run).

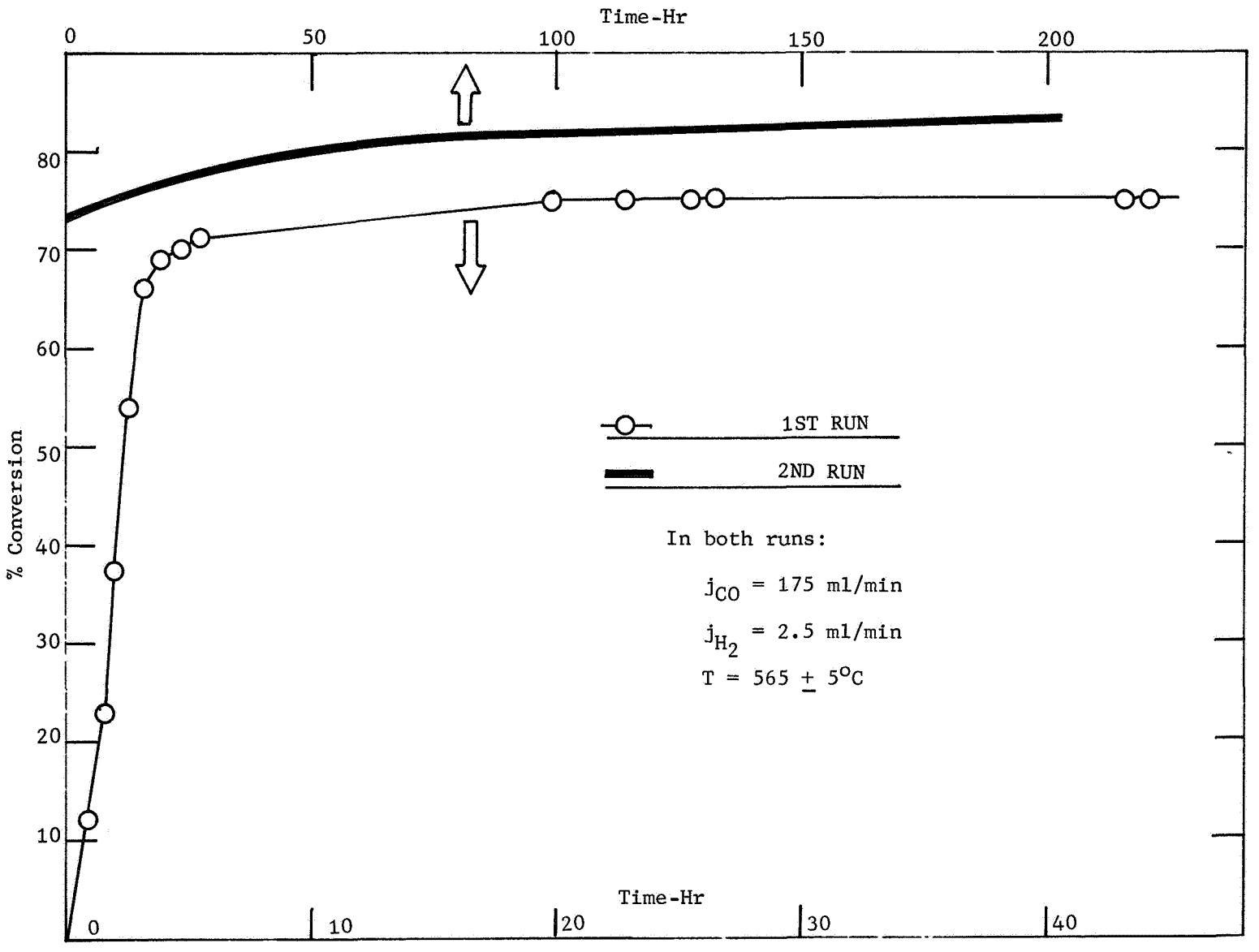

Fig. 4-1 Efficiency of the Steel Reactor as a Function of Exposure Time

Section 5

TESTING

5.1 SINGLE CELLS

AC conductivity measurements were made in air on three hot-pressed zirconia-scandia electrolyte disks having a 20 cm^2 electrode area. A General Radio 1650-B Impedance Bridge at a frequency of 1000 Hz was used. The electrolyte disks used were prepared from Varlacoid zirconia powder containing 7.9 mole% scandia (G-9H, RG-9G) and Tam zirconia powder containing 8 mole% scandia (G-15B). The G-9H, RG-9G, and G-15B disks were of .085, .081, and .076 cm thickness respectively. A schematic drawing of a cell showing the disk, electrodes, current leads and voltage probes is shown in Fig. 5-1. All specific conductivity values have been corrected for lead resistances and are shown on a log conductivity vs. 1/T plot in Fig. 5-2. For comparison, bulk conductivity data are shown by Strickler and Carlson (Ref.10) on zirconia-scandia (6.0 mole% scandia) prepared by cold pressing and sintering, and by Ruka, Bauerle and Hrizo (Ref.11) for 3000 to 5000 Å thin film specimens (10 mole% scandia) prepared by RF sputtering and subsequent sintering. Results of samples G-9H, RG-9G, and G-15B are in good agreement with the Carlson and Strickler bulk data (extrapolated below 650°C) to ~500°C and deviate from the bulk data slope (low activation energy) at lower temperature approaching the thin film data slope (high activation energy) of Ruka, Bauerle and Hrizo (extrapolated below 500°C).

A possible explanation for the conductivity-temperature behavior and change in activation energy for the hot-pressed bulk samples is proposed here. In zirconia-scandia and other mixed oxide solid solutions having the imperfect fluorite structure the number of oxide vacancies or charge carriers has been found to be fixed by the concentration of the added non-reducible lower valent cation and is independent of temperature. This generalization holds true except under severe reducing conditions and with additions of easily reducible cations. For zirconia-scandia solid solutions, therefore, the activation energy contributes only to the motion of oxide vacancies and is a constant. At lower temperatures a large

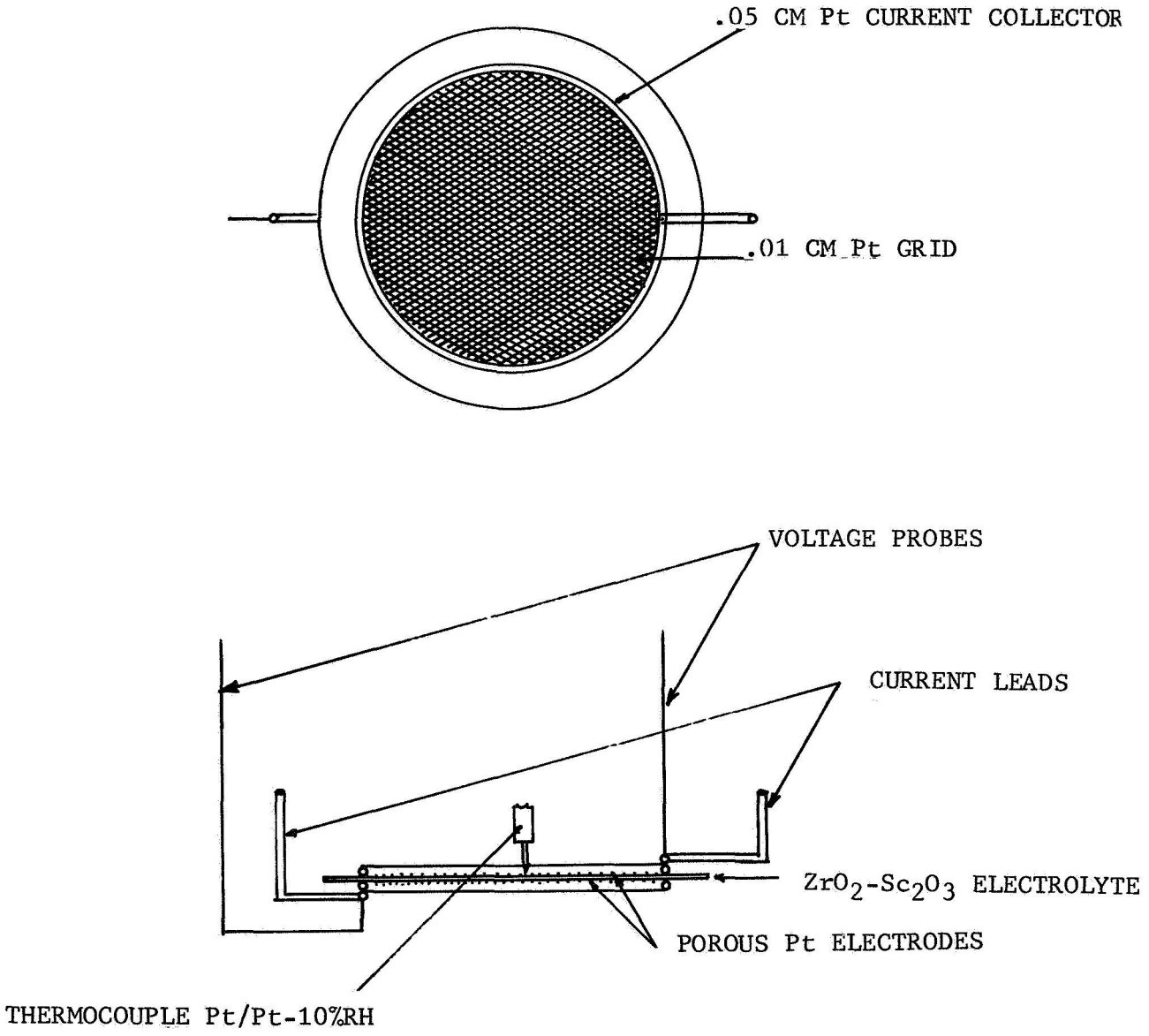

Fig. 5-1 Single Cell Electrical Testing Arrangement

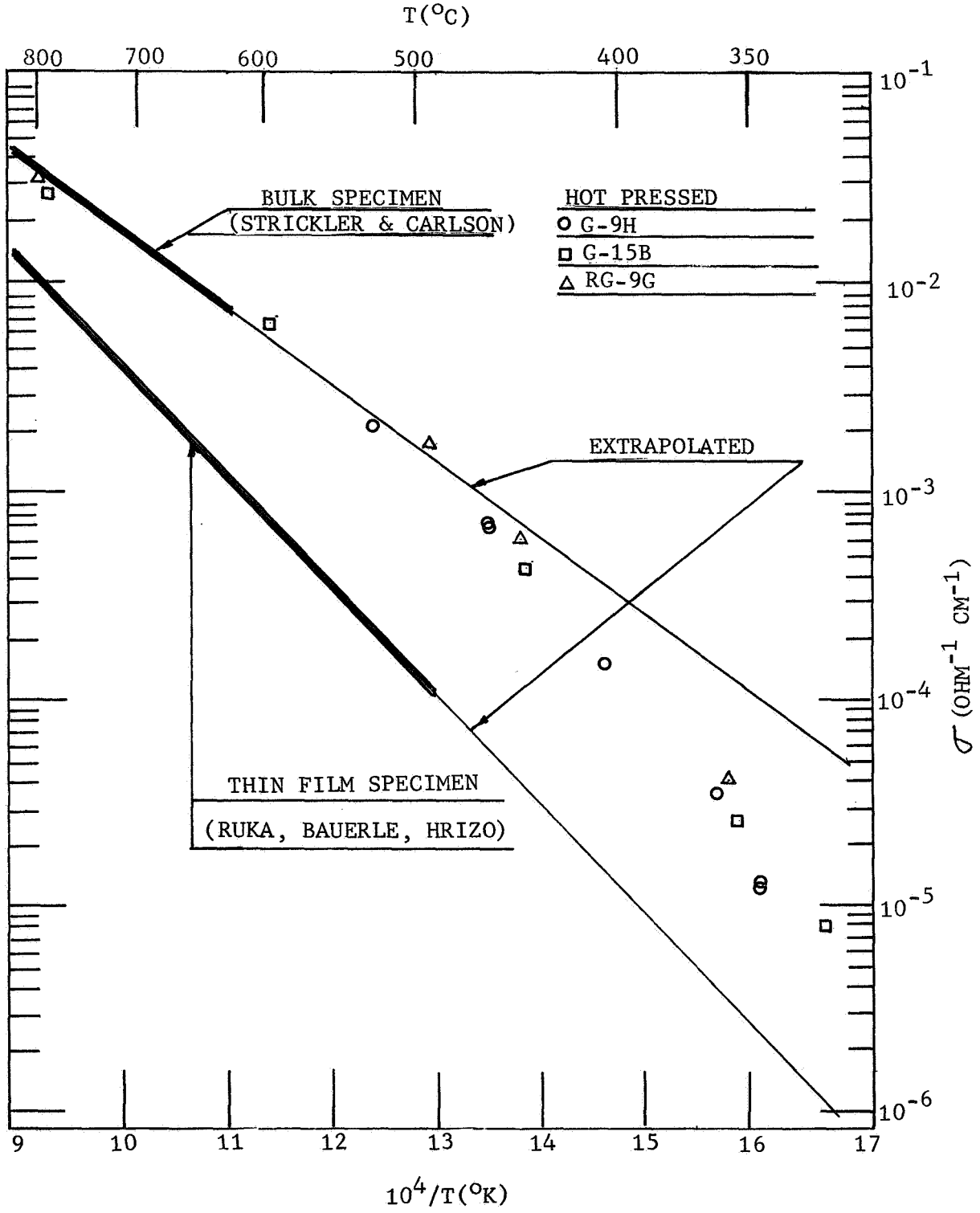

Fig. 5-2 Comparison of Conductivity of Bulk Hot-Pressed, Cold-Pressed and Sintered, and Thin Film Zirconia-Scandia Electrolytes

number of oxide vacancies is trapped at various structural imperfections such as dislocations or by the lower valency cations (scandium)(Ref. 12). Therefore the activation energy of conduction at lower temperatures is a sum of two or more energies consisting of the energy for motion of oxide vacancies and the dissociation energy necessary to free the trapped or complexed oxide vacancies.

It would appear that the thin film oxide has a much smaller concentration of free oxide vacancies throughout the whole temperature range under discussion. In considering thin films vs. bulk samples, the lower specific conductivity of thin films (e.g., a factor of 10 at 500 to 600°C) for the contemplated operating temperature must be taken into consideration.

Current voltage measurements were also made on these cells in air (electrolytic oxygen transfer) at current densities of 200 mA/cm^2 and 4 A total currents in the temperature range 780 to 980°C. A difference in applied voltage for oxygen transfer depending on the direction of current was noted initially. This asymmetrical polarization effect was virtually eliminated with continuous cell operation at high current densities and change of polarity or current direction. Current-voltage curves similar to those obtained here are presented below for each of the cells electrically series connected in the 12-A electrolysis unit. For the individual cells measured here a temperature gradient radially from the center to the outer rim of the electrode of +5°C was found. The voltage drop from the center of the electrode to the outer .05 cm platinum rim at the connecting .10 cm platinum pigtail is $\sim$.03 volt and $\sim$.11 volt for cell currents of 1 A and 4 A at 825 to 850°C. These results indicate the absence of an equipotential surface across the 20 cm^2 electrodes at $I \geqslant 1A$.

5.2 TWELVE-AMPERE ELECTROLYZER

5.2.1 Experimental Details

The preparation of the electrolyte disks and attachment of electrodes and the construction of the 12-A electrolysis unit has been described in detail in Section 3. The elec-

trolyte disks in the cells are of approximate equal thickness of .11 cm. For review of the arrangement of the electrically series-connected cells Figs. 2-5 and 2-6 should be referred to.

After the final sealing operation and cool-down to room temperature, the unit was checked for electrical shorts and infinite resistance was found between all sealed-in platinum .10 cm wire leads. The cells were then connected externally in series by means of the wire leads.

Similarly for review of the parallel gas flow pattern to cathode and anode chambers Figs. 2-1 and 2-5 should be referred to. The three-cell unit has two interchangeable cathode and anode chambers each of which is served by an inlet and outlet manifold and inlet and outlet port hole of .10 cm diameter. The pressure drop across the port holes of each set of chambers was measured with the maximum required flow of 160 to 165 ml/min of CO_2 and found to be $\lesssim$.5 inch of water ($\sim$.02 psi). To check for chamber cross-leakage, one set of gas chambers was connected to a 10 ml bubble meter and 160 to 165 ml/min of gas was flowed through the other chambers and vented at both one atmosphere and at 1 to 2 inches of water above 1 atm. No cross-leakage was evident at the bubble meter. A final leak check was made by immersing the unit in water and pressurizing the inside of the unit to .5 psi above atmosphere with no evidence of leakage to the outside.

After completion of these tests, glass tubes were connected to the zirconia manifold tubes by means of brass fittings and the unit was placed approximately in the center of a 4-inch Kanthal furnace such that the fittings did not overheat (see Fig. 5-3). The general arrangement of the test unit is shown schematically in Fig. 5-4 combined with the CO-disproportionation and C-deposition reactor which will be more fully described below. Fig. 5-5 presents the schematic wiring diagram of the electrolysis unit showing the ohmic resistance losses, voltage probes and current taps. The instruments used in AC and DC electrical measurements are shown in block form in Fig. 5-6.

The furnace is kept at a constant temperature by means of an on-off controller. A Pt/Pt-10%Rh thermocouple (top T.C.) is

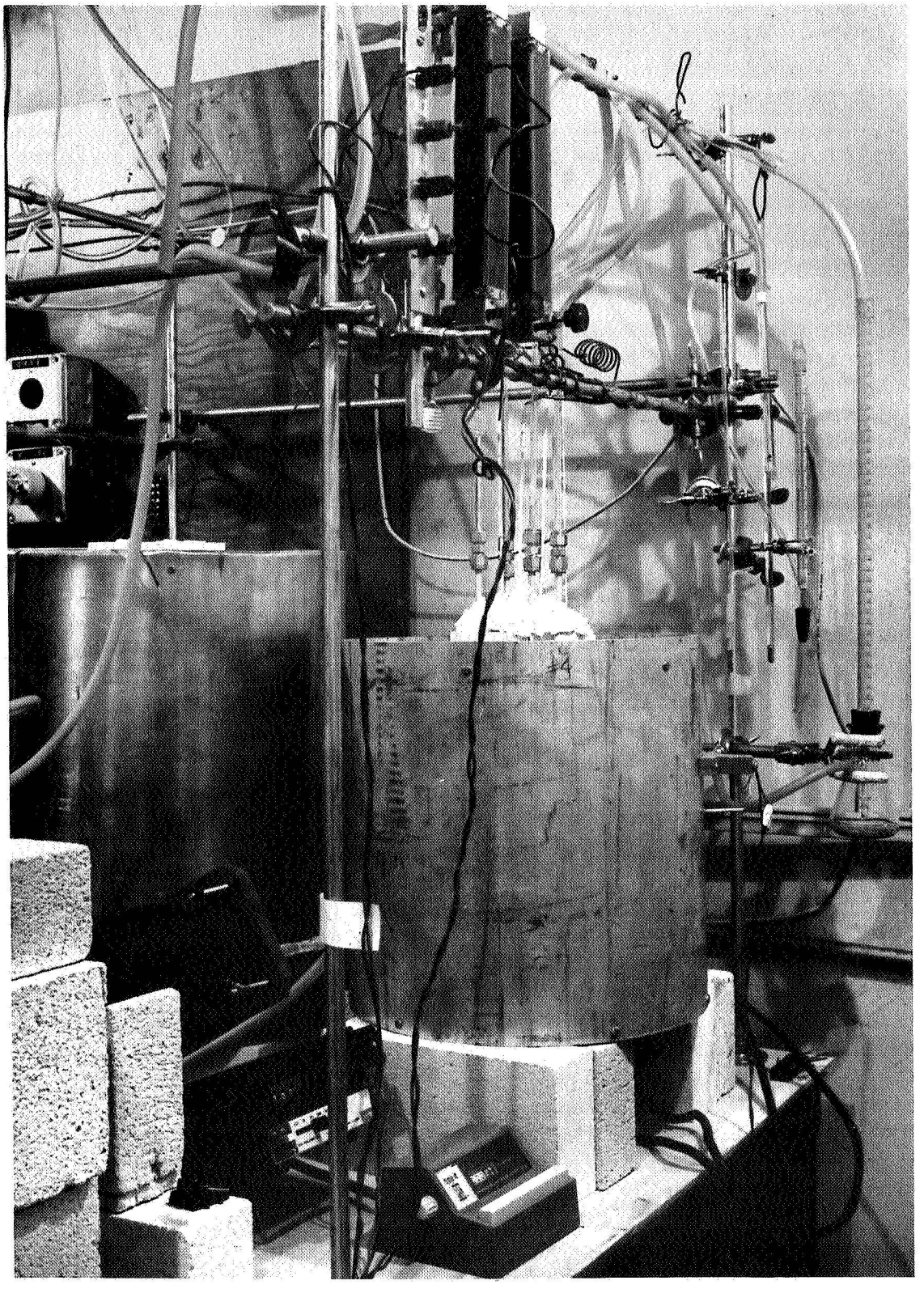

Fig. 5-3 Twelve-Ampere Electrolysis Unit Undergoing Testing

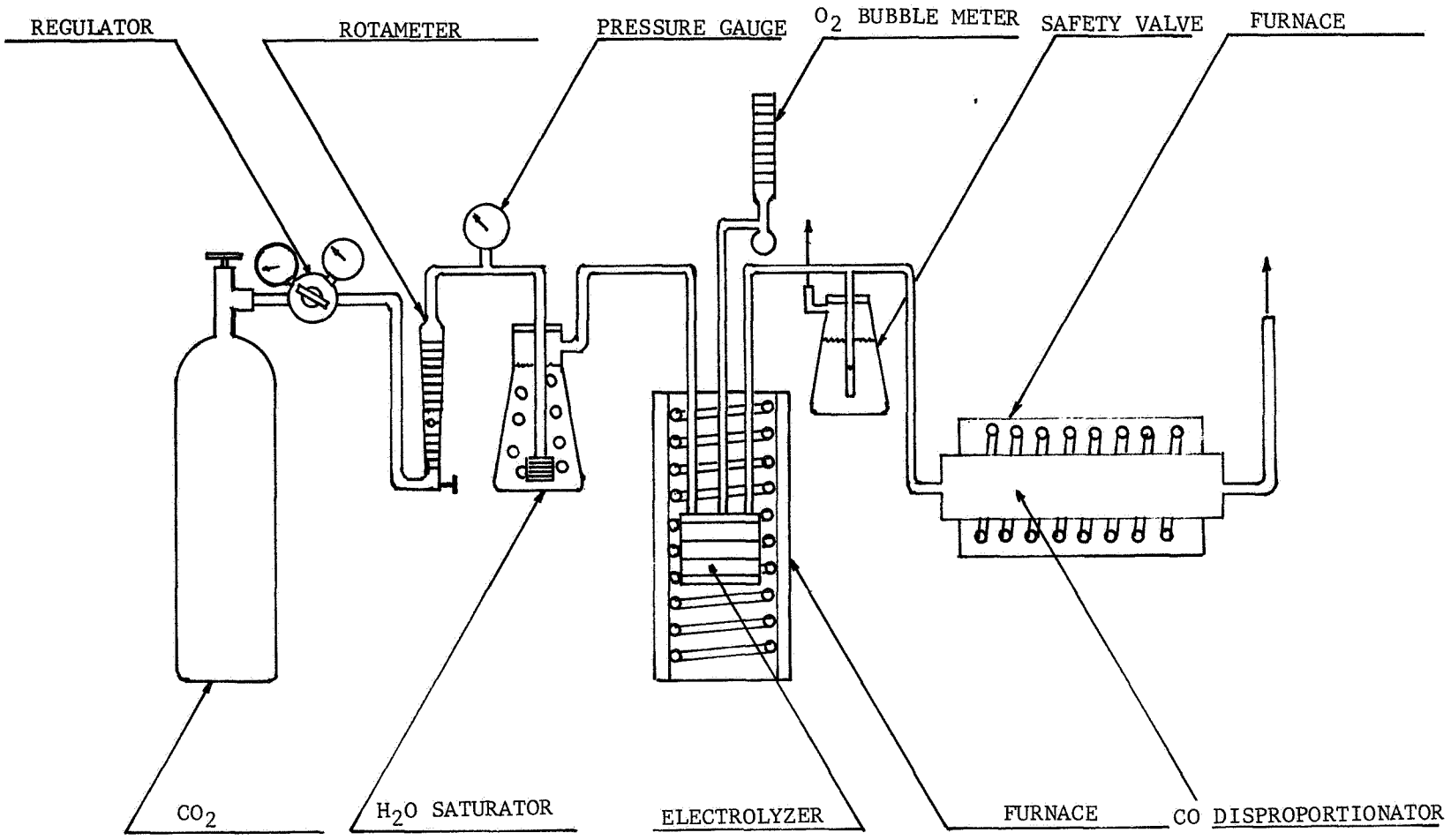

Fig. 5-4 Schematic Diagram of Electrolyzer and Reactor

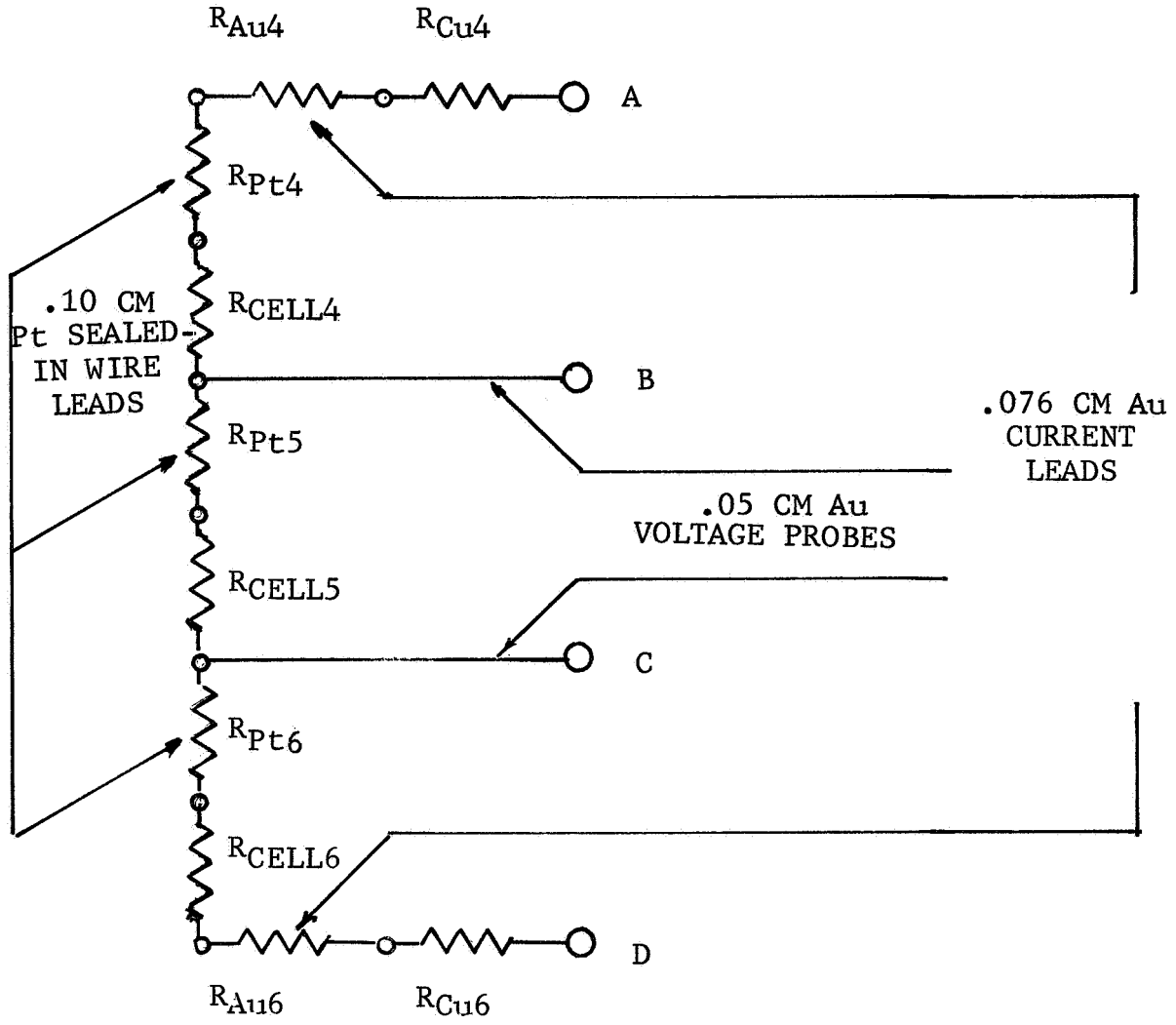

Fig. 5-5 Schematic Wiring Diagram of 12-A Electrolysis Unit

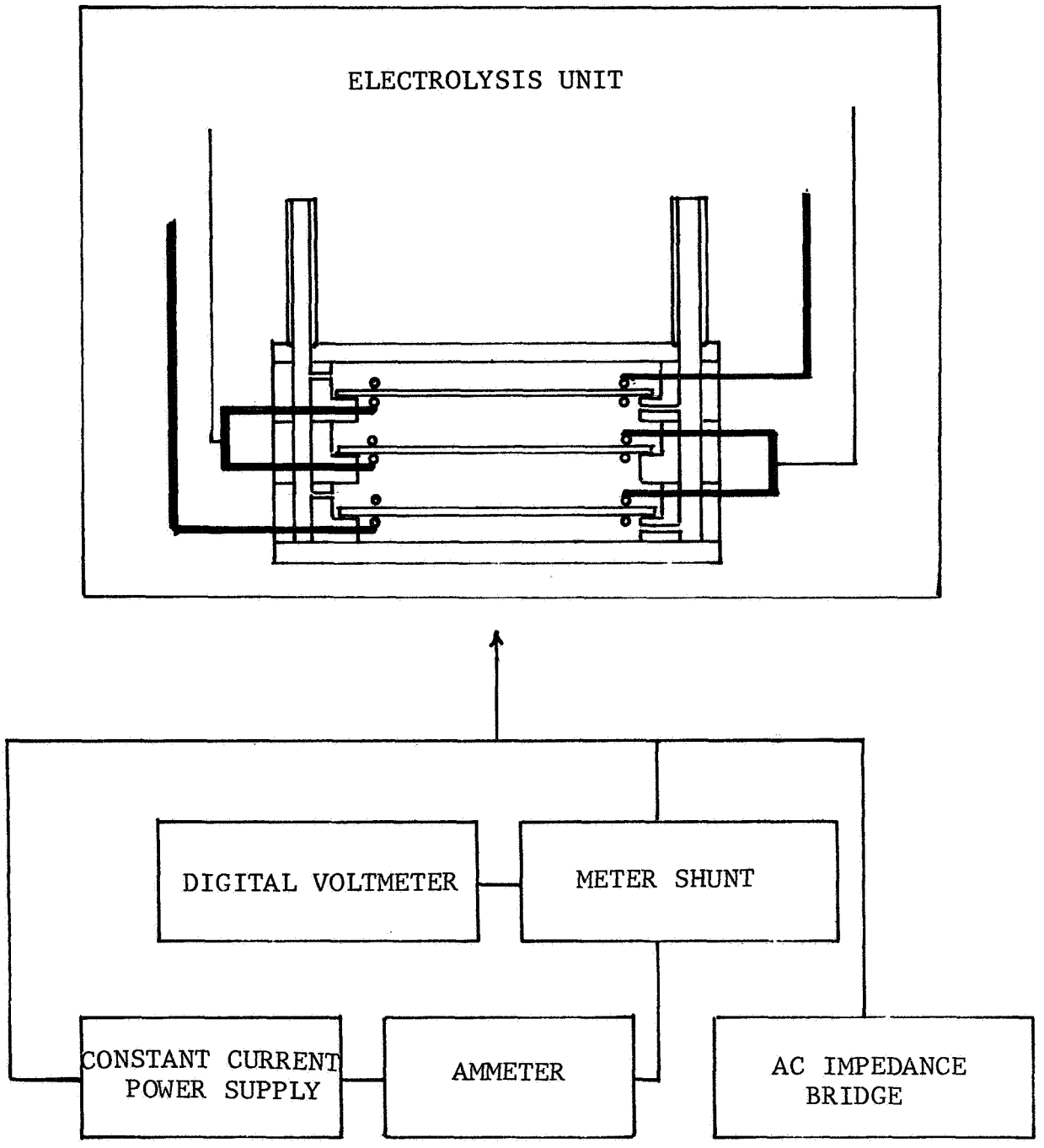

Fig. 5-6 Schematic for Electrical Measurements

located on the upper plate of the unit near a zirconia manifold tube while a second similar thermocouple (bottom T.C.) is located on the outside of the unit near the lower plate. A maximum furnace cycling temperature of 5 to 6 degrees was monitored by these thermocouples. An axial temperature profile of the unit was made by inserting a T.C. inside one of the gas manifolds. With the bottom T.C. at 845°C, the temperatures of the upper (No. 4), middle (No. 5) and lower (No. 6) cells were estimated to be 815, 820 and 825°C $\pm$ 5°C in both the radial and axial directions. The furnace remained at the temperature setting maintained during this calibration for the period of the electrical measurements described below.

5.2.2 Results and Discussion

Electrolytic oxygen transfer. Electrolytic oxygen transfer was undertaken to pretreat electrodes by reversal of polarity at given intervals, and to obtain electrolyzer operating parameters to be used as a basis for comparison with CO_2-H_2O electrolysis under duplicated conditions of temperature gradients, current densities, I^2R heating effects, and resistive lead losses. A comparison of DC (cell resistance) and AC conductivity data and possible polarization losses can also be made. The platinum/oxygen/oxide electrode is ideally suited for this purpose. Cathodic reduction of oxygen and anodic oxidation of oxide ions occur reversibly on a porous platinum surface beyond the range of our maximum used current density of 200 mA/cm^2, according to the reaction:

$$O_2 + 4e \rightleftharpoons 2O^{=} \qquad (5\text{-}1)$$

Oxygen flow through the cathode chambers was maintained at 140 ml/min. Applied voltages measured as a function of current after attainment of steady-state conditions were obtained across the unit and each of the cells in series. These values uncorrected for lead resistance losses are shown in Table 5-1 and plotted for the electrolyzer (three cells in series) in Fig. 5-7. As can be seen from the data in Table 5-1, the voltages of cell 5 are consistently lower than the approximately similar values of the other two cells.

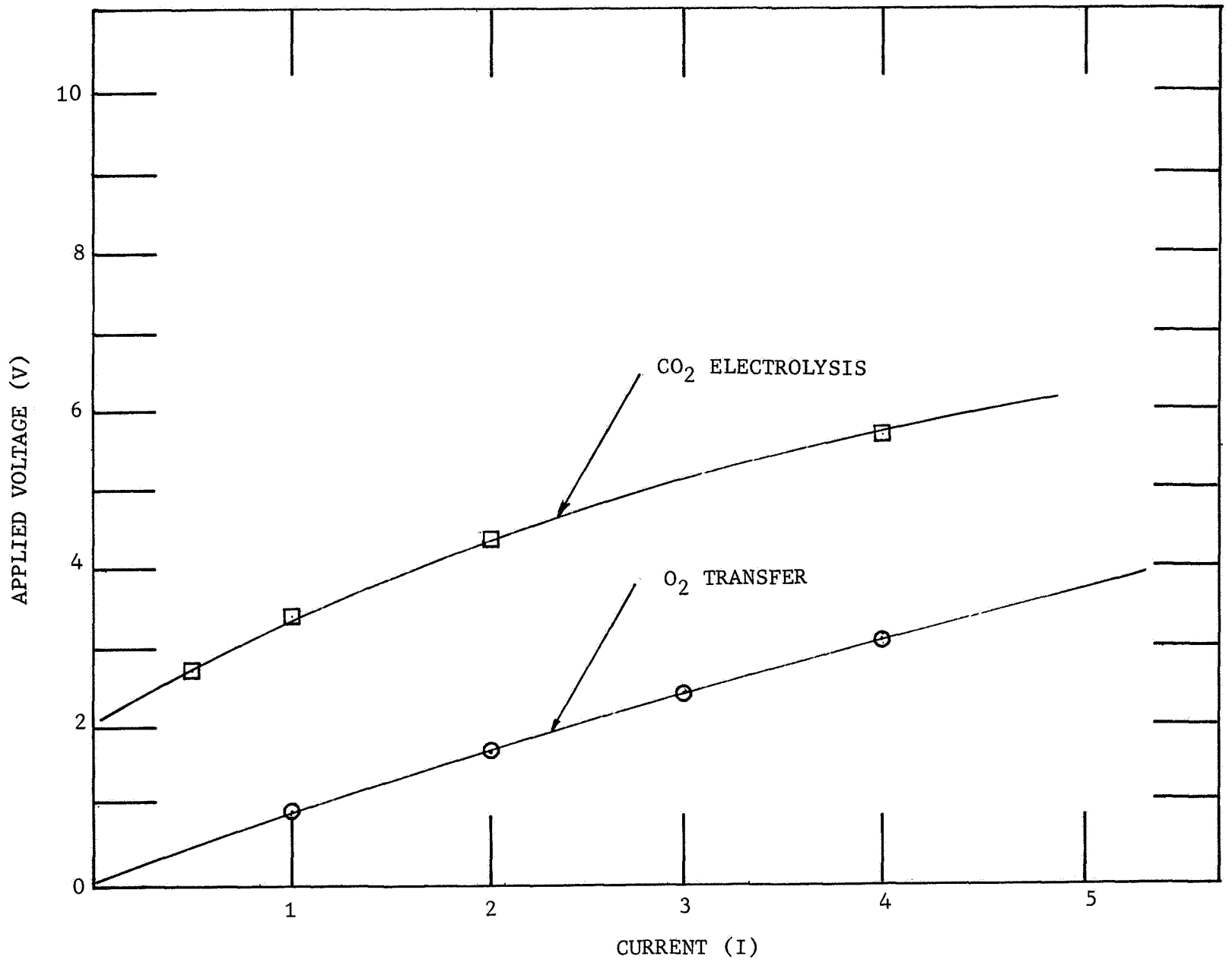

Fig. 5-7 Current-Voltage Curves for Electrolyzer

Table 5-1

CURRENT-VOLTAGE FOR OXYGEN TRANSFER AT 820°C

CURRENT (A)	APPLIED VOLTAGE (V)			
	Total Unit (E_{AD})	Cell 4 (E_{AB})	Cell 5 (E_{BC})	Cell 6 (E_{CD})
1.00	.85	.31	.25	.31
2.00	1.62	.58	.46	.59
3.00	2.33	.82	.64	.85
4.00	2.98	1.07	.80	1.10

Values of the lead resistance losses are presented in Table 5-2. These values are approximate only and were obtained from direct measurement and calculation from wire lengths.

Table 5-2

APPROXIMATE VALUES OF LEAD RESISTANCE LOSSES

RESISTANCE IN OHMS					
INTERNAL	R_{Pt4}		R_{Pt5}	R_{Pt6}	R_{Pt} (TOTAL)
	.07		.06	.07	.19
EXTERNAL	R_{Au6}	R_{Cu6}	R_{Au4}	R_{Cu4}	$R_{Au,\ Cu}$ (TOTAL)
	.04	.02	.04	.02	.13

Correcting for IR lead losses for cells containing electrolyte disks of equal thickness, we conclude from Fig. 5-8 that the applied voltages across each of the series-connected cells are also approximately equal at constant I. From Fig. 5-8 we see that a straight line drawn through the 2 to 4 A region does not extrapolate back to zero voltage. This can be accounted for by a small amount of I^2R heating which lowers

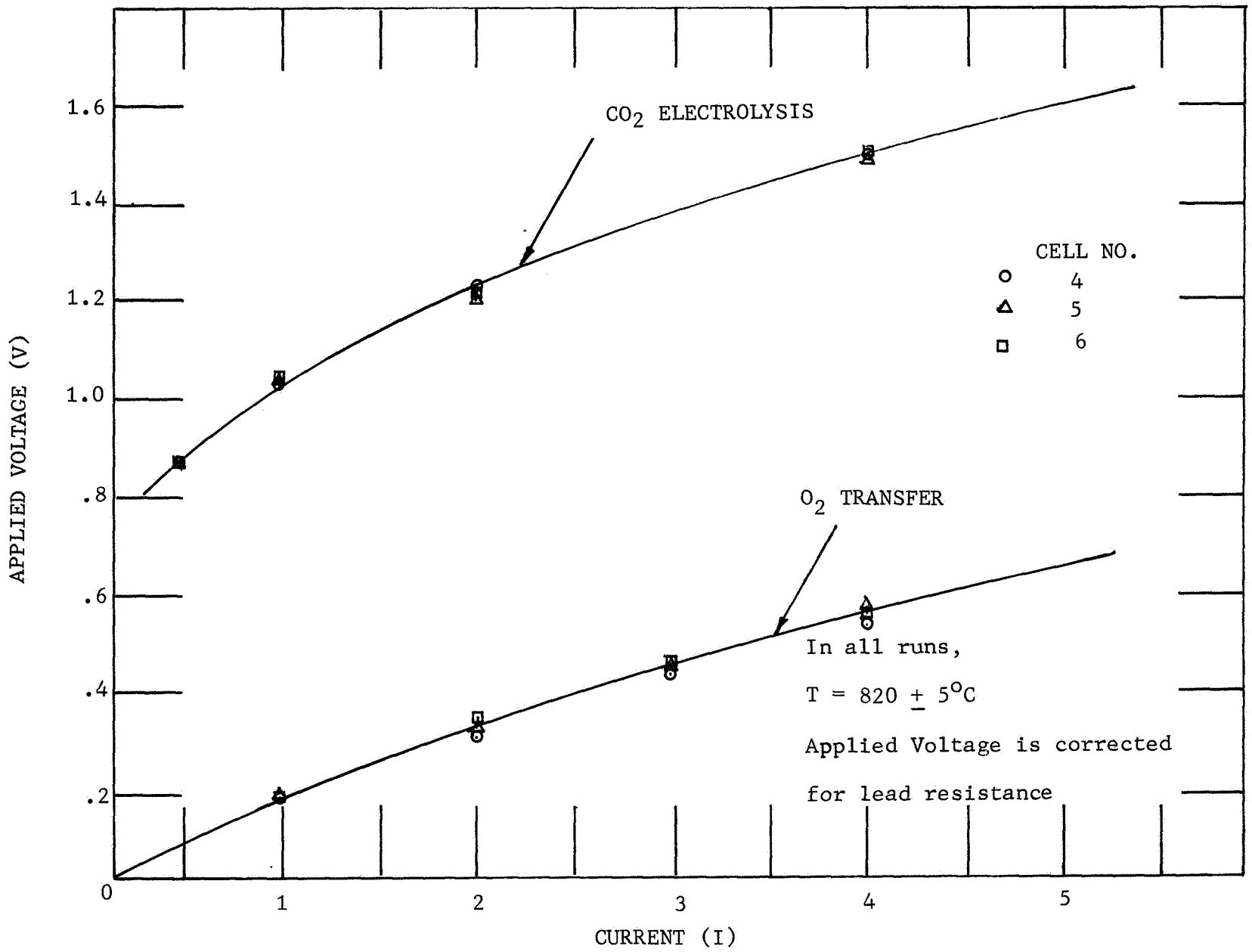

Fig. 5-8 Current-Voltage Curves for Single Cells in Electrolyzer

the resistance of the cells. From the slope we get $R_{DC} \cong .11$ ohms for the combined electrolyte-contact resistance compared to an AC value of $R_{AC} \cong .14$ ohms at open-circuit similarly corrected for lead resistance losses. The values calculated from the AC conductivity-temperature curve for individual cells are $\sim .11$ ohms at 850°C and $\sim .14$ ohms at 820°C. These results point up sharply the relatively high resistance and IR losses of the .10 cm Pt series-connecting lead wires (Table 5-2) in comparison with the 20 cm^2 electrode area cells of .11 cm thickness.

<u>CO_2-H_2O Electrolysis.</u> Before connecting the CO disproportionator to the 12-A electrolyzer, a series of electrical tests was made similar to those carried out in the oxygen transfer experiments. The tests reported here were carried out during a two-week period with the electrolyzer at 24-hr/day continuous operation except for variation of current.

A flow of CO_2 at 160 to 165 ml/min was passed through a water saturator at ambient temperature before entering the electrolyzer. The exit CO/CO_2 stream was vented at atmospheric pressure. A current-voltage curve for three cells in series uncorrected for lead resistance losses is shown in Fig. 5-7. Voltage values were obtained under steady-state conditions and are independent of direction of current. For comparison, the oxygen transfer curve obtained under the same operating conditions is also shown. The applied voltage difference is approximately constant with a value of 2.5 V at 1 A (.85 volt/cell) compared with 2.8 V at 4 A (.93 volt/cell). The theoretical average voltage for the dissociation of CO_2 to CO and O_2 at 820 to 850°C may be calculated from the equation,

$$\bar{E} = E^o + \frac{RT}{2F\Delta n} \sum (n_i \ln p_i - n_f \ln p_f) \qquad (5\text{-}2)$$

where $\bar{E}$ is the average and E^o the standard theoretical voltage, Δn the moles of CO_2 converted to CO and n_i, p_i, n_f, p_f are the initial and final moles and pressures of CO and CO_2. The O_2 evolved at 1 atm. can be neglected here. The difference in applied voltage due to the difference in gas composition of 14%CO at 1 A (three cells in series) versus 55%CO at 4 A can be obtained from the Nernst equation,

$$E = E^o + \frac{RT}{4F} \ln P_{O_2} + \frac{RT}{2F} \ln P_{CO}/P_{CO_2} \qquad (5\text{-}3)$$

A calculation at 825°C gives an applied voltage of ~.88 V for 14% CO at 1 A and ~.98 V for 55% CO at 4 A. An increase in voltage of .10 volt corresponds qualitatively with the results in Fig. 5-7. The small additional cell voltage arising from the effect of an increase in temperature from I^2R heating on the relation between temperature and theoretical voltage as given in Eq. (5-3) may be neglected here.

Several conclusions can be drawn from these results:

(1) The values of the DC resistance per 20 cm^2 cell during CO_2 electrolysis appear to be close to the values obtained for electrolytic oxygen transfer.

(2) Electrode polarization effects at current densities to 200 mA/cm^2 for the cathodic reaction,

$$CO_2 + 2e^- \rightarrow CO + O^= \qquad (5\text{-}4)$$

appear to be low or negligible using the oxygen electrode reaction, Eq. (5-1), as a reference.

(3) The applied voltages corrected for lead resistance losses per series-connected cell are approximately equal (Fig. 5-8).

(4) A negligible voltage difference indicates no gross imbalance between parallel CO_2 gas flows in the cathode chambers and consequent absence of concentration polarization.

The faradaic efficiency for oxygen production (current efficiency) was measured during the CO_2 electrolysis experiments described above. The oxygen evolved electrolytically at the anodes was monitored by means of a 10-ml bubble meter. The theoretically required oxygen flow rate equivalent to 12 A (4 A per cell for three cells connected in series) is 45.6 ml/min (25°C, 1 atm.). Consistently higher flow rates of from 3 to 4 ml/min were found. Similar results were obtained when the cathode and anode chambers were interchanged. Repeated tests for cross-leakage at open circuit and a flow of 160 to 165 ml/min of CO_2 through the cathode chambers at temperature gave no indication of a measurable gas flow at the bubble meter.

Pressurizing the CO_2 outlet stream at 2 to 4 times the pressure drop found across a set of gas chambers gave a leak

rate on the bubble meter of .4 ml/min, a leak insufficient to account for the inter-chamber leakage found with oxygen flowing in the anode chambers.

Analysis of the oxygen stream obtained by electrolysis was carried out by gas chromatography using a syringe technique to sample the gas. The oxygen stream was found to contain 7 to 8% CO_2 by volume at room temperature and pressure. To check whether this leakage effect occurred only during electrolysis, the electrolytically formed oxygen was replaced with tank oxygen flowing at 50 to 60 ml/min. The oxygen stream was again found to contain 7 to 8% CO_2 by volume.

The problem of cross-leakage with gas flowing in the anode and cathode chambers and negligible cross-leakage with gas flowing only in one set of chambers is apparently due to a small inter-chamber leak whose location has not yet been determined. At this stage, the catalytic reactor (steel pipe used in Section 4) was connected to the 12-A electrolyzer as shown in Fig. 5-4 and the integrated unit was placed on life-test. The electrolyzer temperature was raised $\sim 50^{\circ}C$ and is at $875 \pm 10^{\circ}C$ while the reactor temperature is at $565 \pm 10^{\circ}C$. A flow of carbon dioxide of 160 to 165 ml/min is passed through the water saturator and then to the electrolyzer unit where the CO_2 is electrolyzed at 4 A per cell (12 A total). The effluent CO-CO_2 mixture from the electrolyzer then flows through the catalytic disproportionator and is vented at one atmosphere pressure. Analysis of cathode, anode and reactor gas streams is being made periodically. The electrical characteristics of the electrolysis unit are also being monitored.

Section 6

DISCUSSION

The research and development program described in this report resulted in design, fabrication and testing of a 12-A CO_2-H_2O electrolyzer and CO disproportionator. During the course of this work, a number of problems were solved, but areas requiring further development remain before systems based on solid oxide electrolytic cells can attain the reliability required for actual life-support use. The purpose of this section is to summarize the sequence of fabrication and operational steps that were performed during the program, to point out those steps which we believe to be relatively well developed now and those which are not, and to discuss application of the results of the program to future development of larger units.

6.1 SUMMARY OF THE DEVELOPMENT PROGRAM

The sequence of steps involved in fabrication and testing of the 12-A electrolyzer and catalytic reactor was as follows:

(1) Preparation of stabilized zirconia powder

(2) Hot pressing of 6.35 cm diameter ceramic slugs

(3) Slicing disks from the slugs

(4) Polishing the disks

(5) Plating the disks for sealing

(6) Application of electrodes and grids

(7) Diamond machining cell bodies from ceramics

(8) Plating the bodies for sealing

(9) Furnace brazing disks to bodies to form individual cells

(10) Leak checking each cell

(11) Diamond machining and plating end plates

(12) Conicalizing and plating ends of ceramic tubes

(13) Furnace brazing four tubes to top plate and leak checking

(14) Furnace brazing bottom plate, three cells and top plate with tubes together to form 12-A unit

(15) Checking for both internal and external leaks at room temperature

(16) Making electrical connections

(17) Setting up the electrolyzer in a furnace and leak checking at high temperature

(18) CO_2-H_2O electrolysis testing

(19) Construction of iron catalytic reactor

(20) Pre-treatment of the reactor

(21) Connection of the electrolyzer and the reactor and operation of both

6.2 PRESENT STATE OF THIS TECHNOLOGY

Fabrication, by hot pressing, of 6.35 cm diameter scandia-stabilized zirconia disks and application of platinum electrodes proceeded satisfactorily to give electrolytic cells of high ionic conductivity which met the operating requirements of the 12-A unit for CO_2-H_2O electrolysis. Diamond drilling, grinding and polishing of both the disks and ceramic bodies has been developed sufficiently to produce the desired dimensions and surface finish. The cleaning, sensitizing and plating procedures yield uniform precious metal deposits compatible with the ceramic substrates and of adequate thickness and adhesion for the sealing process. The precious metal brazing technique using alloys gives reliable high-

temperature wire, body-to-body, and conical seals, but is less reliable at this point for the disk-to-body (ledge) seals. The validity of the basic design concepts (see Section 2) has been reinforced by this fabrication and testing program. However, the shape and dimensions of the zirconia bodies present serious fabrication problems. In addition, behavior of the ledge seals upon rapid temperature cycling and other testing gave some indication that this body geometry adversely affected these seals. The bodies used for the construction of this 12-A unit were not intended as the optimum in shape, wall thickness or weight but were used for convenience in fabrication, as described in Section 2.

The conclusion that solid oxide electrolytic cells are the most promising route for oxygen recovery from carbon dioxide for long duration space missions was reached by the Hamilton Standard Division of United Aircraft Corporation under a NASA-funded review of aerospace life-support systems (Ref. 13). The performance of the 12-A prototype unit described above would appear to add further weight to this conclusion. It is also of interest to note that Prof. L. G. Austin of North Carolina State University in a NASA-funded review of government-supported fuel cell research stated, in reference to solid oxide fuel cells, that "...the mechanical problems of making plate cells and stacks will have to be solved." (Ref. 14) We feel that this statement is equally valid for solid oxide electrolyzers and that the techniques now being developed will lead to solutions of these problems.

The work to date has developed important elements of high-temperature solid oxide electrolyte technology such as the large ceramic electrolyte disks, electrodes, seals, manifolding, and electrical leads passing through the ceramic to the electrodes. Although additional development work is needed in some of these areas, particularly the disk-to-body seals and better fabrication methods for the bodies, the basic processing steps for making the parts and assembling them together are reasonably adequate. In contrast, no significant effort has been made to optimize engineering parameters, such as body shape, wall thickness and weight, in a quantitative way. For example, the weight of the present 12-A unit is approximately 1.5 pounds, which, if the same methods were used, would lead to a weight of 15 pounds for a one-man unit operating at 200 mA/cm^2. Eliminating unnecessary ceramic by reducing thicknesses is estimated to allow the weight to

be cut to one half or one third of this value. Weight data are summarized in Table 6-1 for the present 12-A unit with three cells having a total area of 60 cm^2 operated at a current density of 200 mA/cm^2, and also for a 12-A unit containing six cells with a total area of 120 cm^2 operated at 100 mA/cm^2. If the six-cell unit were operated at 200 mA/cm^2, it would have an oxygen output equivalent to 24 A for its weight of 2.3 pounds or approximately 12 pounds for an electrolyzer of one-man capacity.

Table 6-1

WEIGHTS OF 12-A UNIT COMPONENTS

COMPONENT	WEIGHT OF EACH (Grams)	12-A ELECTROLYZERS 3-CELL, 200mA/cm^2 No.	Total Weight (Grams)	6-CELL, 100mA/cm^2 No.	Total Weight (Grams)
Electrolyte Disk (6.35 cm diam. x .127 cm thick)	24				
Disk with electrodes and leads	27	3	81	6	162
ZrO_2 tube (.6 cm diam. x 22 cm long)	16.5 (.75 g/cm)	4	66	4	66
ZrO_2 End Plate	110	2	220	2	220
ZrO_2 Cell Body	100	3	300	6	600
			667		1,048

The dimensions of the 12-A unit are 2.75 x 2.75 x 2.0 inches not including the four gas tubes and the 2.0 inch length could be reduced but not the other dimensions if 2.5 inch diameter disks are used. Further work in this field can now begin to give attention to engineering aspects.

6.3 FUTURE DEVELOPMENT

Further development of solid oxide electrolyte CO_2-H_2O electrolyzers for aerospace life-support applications, based on the progress reported above, should retain the basic design principles herein discussed. Additional work needs to be done to improve the reliability of the disk-to-body seals, to enable easier fabrication of the bodies, and to consider optimizing various dimensional and operational parameters. Modifications of body shape could contribute toward all of these goals. The results of these studies should then be applied to constructing a larger unit.

The problems that were experienced with disk seals, but not with the other three sealing geometries, seem to be intimately involved with the shape, dimensions and compositions of the bodies. Improvement of these seals would, therefore, be closely associated with development of improved bodies and of better fabrication techniques. Compositions other than partially stabilized ZrO_2-CaO should be considered and extension of hot pressing from ZrO_2-Sc_2O_3 disks to larger sizes and other body geometries with ZrO_2-CaO and ZrO_2-Y_2O_3 would be possibilities.

Consideration should be given to a number of engineering aspects of these units in a quantitative or semi-quantitative way. Included among these would be stress-strain relationships for each specific body shape and body-cell sub-unit, optimum gas channel sizes, current density, operating temperature, and outlet CO/CO_2 ratio. The latter two parameters would be determined by the requirements of the CO disproportionator as well as by those of the electrolyzer. Based on data thus developed, a one-man capacity (127-A) electrolyzer consisting of modules, each of which contains at least six cells, should be built and tested.

Section 7

REFERENCES

1. J. Weissbart and W. H. Smart, "Study of Electrolytic Dissociation of CO_2-H_2O Using a Solid Oxide Electrolyte," NASA Contractor Report CR-680, February, 1967

2. J. Weissbart and W. H. Smart, "Study of Electrolytic Dissociation of CO_2-H_2O Using a Solid Oxide Electrolyte," Second Annual Report, Contract NAS2-2810, Lockheed Missiles and Space Co., Palo Alto, California, August, 1967

3. J. Weissbart, W. H. Smart and T. Wydeven, Aerospace Medicine, 40, 136 (1969)

4. R. C. Rossi and R. M. Fulrath, J. Am. Ceram. Soc., 48, 558 (1965)

5. F. R. N. Nabarro, Rept. Conf. Strength of Solids (Univ. Bristol), July, 1947, p. 75

6. C. Herring, J. Appl. Phys., 21, 437 (1950)

7. P. L. Walker, Jr., J. F. Rakszawski and G. R. Imperial, J. Phys. Chem., 63, 140 (1959)

8. A. J. Glueckert and G. A. Remus, General American Research Division, General American Transportation Corporation, GARD Report 1288-6080, 1967

9. L. A. Haas, S. E. Khalafalla and P. L. Weston, Jr., Bureau of Mines Report 7064, 1968

10. D. W. Strickler and W. G. Carlson, J. Am. Ceram. Soc., 48, 286 (1965)

11. R. J. Ruka, J. E. Bauerle and J. Hrizo, "Study of Thin Layer Oxide Electrodes and Electrolytes," Contract Nobs-94295, Westinghouse Research Laboratories, Pittsburgh, Pennsylvania, June, 1968

12. F. Kroeger, J. Am. Ceram. Soc., 49, 215 (1966)

13. "Trade-Off Study and Conceptual Designs of Regenerative Advanced Integrated Life Support Systems (AILSS)," Contract NAS1-7905 Final Report, Hamilton Standard Division of United Aircraft Corporation, December, 1968

14. L. G. Austin, "Fuel Cells, A Review of Government-Sponsored Research, 1950-1964," NASA SP-120, 1967, p. 132